Journal of Controlled Release 369 (2024) 404–419

Contents lists available at ScienceDirect

Journal of Controlled Release

journal homepage: www.elsevier.com/locate/jconrel

Cryogel microcarriers for sustained local delivery of growth factors to the brain

Abrar Hakami [a,b,1], Kaushik Narasimhan [c,1], Giulia Comini [c], Julian Thiele [d,e], Carsten Werner [d], Eilís Dowd [c,*], Ben Newland [a,*]

[a] School of Pharmacy and Pharmaceutical Sciences, Cardiff University, King Edward VII Avenue, Cardiff CF10 3NB, UK
[b] Department of Pharmaceutics, Faculty of Pharmacy, King Abdulaziz University, Jeddah 21589, Saudi Arabia
[c] Pharmacology & Therapeutics and Galway Neuroscience Centre, University of Galway, H91 W5P7 Galway, Ireland
[d] Leibniz-Institut für Polymerforschung Dresden e.V., 01069 Dresden, Germany
[e] Institute of Chemistry, Otto von Guericke University Magdeburg, 39106 Magdeburg, Germany

ARTICLE INFO

Keywords:
Cryogel microcarrier
Growth factors
Sustained release
Microfluidics

ABSTRACT

Neurotrophic growth factors such as glial cell line-derived neurotrophic factor (GDNF) and brain-derived neurotrophic factor (BDNF) have been considered as potential therapeutic candidates for neurodegenerative disorders due to their important role in modulating the growth and survival of neurons. However, clinical translation remains elusive, as their large size hinders translocation across the blood-brain barrier (BBB), and their short half-life *in vivo* necessitates repeated administrations. Local delivery to the brain offers a potential route to the target site but requires a suitable drug-delivery system capable of releasing these proteins in a controlled and sustained manner. Herein, we develop a cryogel microcarrier delivery system which takes advantage of the heparin-binding properties of GDNF and BDNF, to reversibly bind/release these growth factors *via* electrostatic interactions. Droplet microfluidics and subzero temperature polymerization was used to create monodisperse cryogels with varying degrees of negative charge and an average diameter of 20 μm. By tailoring the inclusion of 3-sulfopropyl acrylate (SPA) as a negatively charged moiety, the release duration of these two growth factors could be adjusted to range from weeks to half a year. 80% SPA cryogels and 20% SPA cryogels were selected to load GDNF and BDNF respectively, for the subsequent biological studies. Cell culture studies demonstrated that these cryogel microcarriers were cytocompatible with neuronal and microglial cell lines, as well as primary neural cultures. Furthermore, *in vivo* studies confirmed their biocompatibility after administration into the brain, as well as their ability to deliver, retain and release GDNF and BDNF in the striatum. Overall, this study highlights the potential of using cryogel microcarriers for long-term delivery of neurotrophic growth factors to the brain for neurodegenerative disorder therapeutics.

1. Introduction

In the realm of neurodegenerative disorders, the absence of effective disease-modifying treatments stands as a formidable challenge, underscoring the pressing need for innovative therapeutic approaches. Neurotrophic growth factors such as glial cell line-derived neurotrophic factor (GDNF) and brain-derived neurotrophic factor (BDNF) have garnered attention due to their important role in modulating growth and repair of neurons in the brain [1,2]. For example, GDNF has long been under investigation as a potential therapy for Parkinson's disease (PD) [3]. Moreover, BDNF has been used to guide neuronal differentiation of stem cells and stimulate axonal growth as potential therapies for other neurological disorders [4]. Growth factors would create a supportive environment for the existing neurons, possibly slowing down or stopping the disease progression and relieving some of the symptoms associated with PD [5,6]. In addition, the synergistic co-administration of growth factors with emerging cell-transplantation therapies could potentially support the survival and maturation of grafted cells thus maximizing the efficiency of such therapies [7,8].

However, growth factors are proteins that have a relatively large

* Corresponding authors.
E-mail addresses: eilis.dowd@universityofgalway.ie (E. Dowd), newlandb@cardiff.ac.uk (B. Newland).
[1] *These authors contributed equally.*

https://doi.org/10.1016/j.jconrel.2024.03.023
Received 15 December 2023; Received in revised form 5 March 2024; Accepted 14 March 2024
Available online 4 April 2024

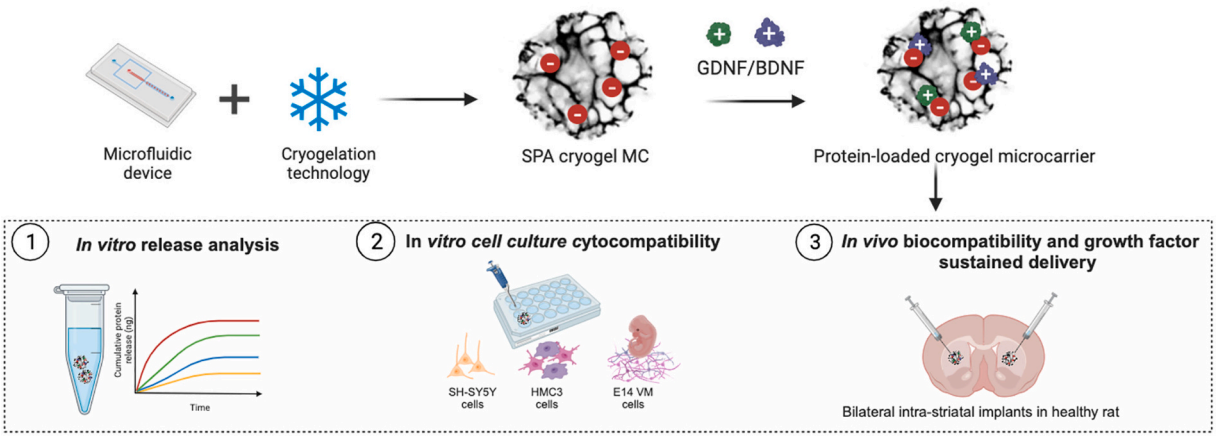

Fig. 1. Schematic illustration/overview of the experimental approach to synthesis of SPA cryogels microcarriers to be used for *in vitro* release analysis and biological studies *in vitro, and in vivo,* Created with BioRender.

molecular weight, making them unable to cross the blood-brain barrier (BBB) and reach the target area in the brain. Moreover, they have a short half-life *in vivo*, thus requiring repeat administration. For example, the half-life of GDNF is approximately 34 h in cerebrospinal fluid [9] and 3–4 days in the brain [10]. To address these challenges, several potential delivery systems for neurotrophic growth factor delivery have been developed in the treatment of PD such as direct infusion of the growth factor into the brain and *ex vivo* gene therapy [11,12]. Nevertheless, the issue of delivery and getting a sustained release of growth factors over a suitable duration remains one of the main hurdles for their clinical translation into a treatment of PD [13,14].

One approach that has been widely investigated is using injectable polymeric biomaterials as controlled delivery systems to protect the encapsulated growth factors and release them slowly over time within the diseased region of the brain [15,16]. Among these biomaterials, microspheres have emerged to improve growth factor delivery to the brain. For example, Garbayo et al. demonstrated the neuroprotective effect of GDNF-PLGA microspheres in rat [17] and monkey [18] models of PD. They reported that a sustained GDNF level in the brain provided motor improvement and dopaminergic function restoration. *In vitro* release studies of the neurotrophic factor with rodent models indicated that around 70% of the total GDNF was released within 40 days. While in the monkey model, a total of around 80% of GDNF was released within 20 days followed by ~10% being released slowly over the following 40 days. One shortcoming of microsphere-based systems is therefore the initial burst release where the protein diffuses rapidly through the polymer within the first days [19].

Hydrogel biomaterials have also been used extensively to deliver growth factors to the brain. For instance, Moriarty et al. demonstrated that encapsulating grafts of cells obtained from the embryonic ventral mesencephalon (VM) in a GDNF-loaded collagen hydrogel resulted in increased survival of dopaminergic neurons in the graft, enhanced striatal reinnervation, and improved motor function in 6-OHDA lesion rats [7,20]. However, due to the highly porous/hydrated nature of the hydrogel alongside the partial enzymatic degradation of the hydrogel, GDNF is released quickly, with significant depletion of GDNF in the rat striatum by day 4 post-transplantation [20].

Designing new delivery systems to control growth factor release locally in the brain is still challenging. Herein, we investigate the use of cryogel microcarriers. Cryogels are a class of biomaterial characterized by a macroporous structure and shape-memory properties [21]. They can be soft and spongy, but also robust, and reversibly hydrated/dehydrated without losing mechanical integrity making them a suitable injectable material for brain drug delivery [22]. Cryogelation is a simple strategy that allows the formation of interconnected macroporous cryogels by the crosslinking polymerization of monomers in a frozen solvent, usually water, at sub-zero temperatures [23]. Ice crystal formation serves as a porogen (pore forming agent) during polymerization. The physicochemical and mechanical properties of cryogels can be controlled by changing several parameters of the cryogelation process such as the freezing temperature/rate, initiator used, and the monomer type and content [24]. Therefore, cryogels can be produced with a broad variety of morphologies and properties to suit a particular application.

Since GDNF and BDNF both show heparin binding properties [25,26], we proposed that they could be delivered through affinity-based binding to a cryogel delivery system. In this work, we postulated that by mimicking heparin, negatively charged synthetic cryogel microcarriers would be able to bind GDNF/BDNF electrostatically and reversibly, releasing them in a controlled manner over months. We hypothesized that we could not only control release rates *via* tailoring the charges, but such a system would also hold the potential to be reloadable/refillable. We aimed to develop a platform technology for the controlled local delivery of growth factor to the brain from which novel therapeutic entities can be developed.

Negatively charged cryogel microcarriers were produced from 3-sulfopropyl acrylate (SPA) and poly (ethylene glycol) diacrylate (PEGDA) *via* a microfluidic device. GDNF and BDNF could be loaded to the microcarriers and released in a controlled manner over weeks and months. The microcarriers could also be refilled with GDNF to continue releasing the protein with a similar profile to that of the first release analysis. The microcarriers were cytocompatible towards neuronal, microglial and primary neuron cell types *in vitro*, and were also biocompatible after intra-striatal injection into the healthy rat brain. Finally, microcarriers delivered both GDNF and BDNF to the surrounding brain parenchyma 14 days post-administration by which time neurotrophins injected without a delivery system were no longer detected. A diagram depicting the process of the overall study is shown in Fig. 1.

Table 1
Composition of the various ratio of PEGDA:SPA (10% *w/v*) used for cryogel synthesis in a final volume of 1 mL.

% of SPA content in cryogel microcarrier	Molar ratio, (SPA: PEGDA)	PEGDA (g)	SPA (g)
5%	0.053:1	0.0983	0.0017
20%	0.25: 1	0.0923	0.0077
40%	0.66: 1	0.082	0.018
60%	1.5: 1	0.067	0.033
80%	4: 1	0.043	0.057
95%	19: 1	0.0137	0.0863

2. Materials and methods

2.1. Cryogel microcarrier preparation

A water-in-oil emulsion was used to create sulfonated cryogel microcarriers. The first step was to form droplets then crosslink them at sub-zero temperatures to produce porous cryogels. The precursor/pre-polymer solution, containing polyethylene glycol diacrylate (PEGDA, M_n 700, from Merck # 455008) and 3-sulfopropyl acrylate potassium salt (SPA, from Merck # 31098–20-1) were mixed at differing molar ratios as shown in Table 1 below accompanied with 2 mg/mL of a PEGylated Irgacure 2959 (synthesized *via* the previously published protocol [27]) as a photoinitiator, and 0.05% *v*/v of iFluor™ 647 maleimide (Stratech # 1131944) solution of 10 mg/mL (stored at −20 °C) as a fluorescent probe. All components were dissolved in deionized water and vortexed to be used as the discontinuous phase (water phase). The continuous phase (oil phase) was formed using home-made perfluoropolyether-polyethylene glycol (PFPE-PEG-PFPE), (an ABA triblock copolymer surfactant as described in [28]) (2% *w/v*) acting as a surfactant in Novec™ 7500 hydrofluoroether engineered fluid (HFE-7500, 3 M™, Fluorochem Limited # F051243-1KG). A microfluidic device (Fluidic 947, Microfluidic ChipShop, Germany # 10001336) with a T-junction size of 20 μm was used to generate droplets. Both discontinuous and continuous solutions were transferred into 3 mL syringes with needles. These syringes were connected by polyethylene tubes in combination with a silicone sleeve that connected *via* Male Mini Luer fluid connectors to each of the inlets of both phases on the microfluidic device. The soft silicone sleeves allowed interconnection of relatively hard tubing with the Mini Luer fluid connectors. The flow rate was set at 400 μL/h for the continuous phase and 150 μL/h for the discontinuous phase using syringe pumps (Landgraf Laborsysteme LA30). Then, the resulting emulsion was collected and immersed into a − 60 °C ethanol cooling bath unit overnight (temperature control achieved *via* a Huber, TC100E). The falcon tubes containing the emulsion droplets were submerged on an equal level and a magnetic stirrer was used to circulate the ethanol for more uniform temperature distribution. The next day, the frozen droplets were irradiated with UV light (Omnicure S1500, Excelitas, 23 W/cm^2, 365 nm) within the cooling bath for 3 min to allow the crosslinking of the droplets and formation of cryogel microcarriers.

2.2. Cryogel microcarrier purification

The purification method was adapted from M.J. Männel et al. [26]. Initially, the collection solution that contained the ABA surfactant dissolved in HFE-7500 was removed from the bottom of the tube. 300 μL of a demulsification solution composed of 20% v/v 1*H*,1*H*,2*H*,2*H*-perfluoro-1-octanol (PFO, Merck # 370533-25G) dissolved in HFE-7500 were added to break the emulsion that had been formed. Then, the PFO solution was removed and replaced with another 300 μL of fresh PFO solution (three washing steps). Next, to remove PFO from the solution, three washing steps were done using HFE-7500 oil only. Then, the samples were resuspended in 300 μL water to prevent the aggregation of cryogels. To completely get rid of the oil within the samples, three washes were done with 1 mL acetone (Fisher Scientific #10162180). After that, the samples were washed with ethanol (Fisher Scientific #10437341) three times. To determine the final concentration of the cryogel microcarriers in suspension, a small volume was removed and dried in a pre-weighed 1.5 mL centrifuge tube. This sacrificed (and later discarded) amount gave the mass of cryogels in a known volume, therefore determining the concentration of the stock suspension. Finally, the cryogels were washed three times with deionized water and kept in as suspension in water.

2.3. Cryogel microcarrier characterization

The samples were analyzed before and after the cryogelation *via* light microscopy (Zeiss Primovert) which was equipped with a 10× and 20× objective and a Phantom Miro C110 high-speed camera. Images were taken using the Phantom Camera Control (PCC) software, version 2.8, and then characterized using FIJI ImageJ (National Institutes of Health, NIH) software for size measurement. The size distribution was calculated *via* measuring the diameter of 100 cryogel microcarriers. Cryogels were fluorescently labeled with iFluor™ 647 maleimide during the cryogel microcarrier synthesis. Confocal laser scanning microscopy (Leica TCS SP5) with 633 nm lasers was used to visualize the cryogel microcarrier's size and pore structure in the hydrated state. Images were taken with either 20× air objective, 40 × 1.25NA oil objective, or 100 × 1.4NA oil objective. Fourier transform infrared spectroscopy (FTIR, IRSpirit Shimadzu) of cryogel microcarriers was obtained in the 800–2000 cm − 1 frequency range (MCT-detector, resolution = 4 cm-1, 100 scans per measurement). The spectrum of the PEGDA and SPA monomers was used as a reference.

2.4. Growth factor loading and release analysis in vitro

Cryogel microcarrier loading was performed in protein LoBind Eppendorf tubes (Fisher Scientific # 10708704). First, all tubes were blocked using a blocking solution (PBS +1% bovine serum albumin (BSA) + 0.04% ProClin™ 300, Sigma # 48914-U) for at least two hours to prevent protein adsorption. Loading solutions were prepared to contain either 100 ng, 500 ng, 1000 ng, or 2000 ng of GDNF (Human GDNF, Cambridge Bioscience # GFH2–100) or BDNF (Human BDNF, Cambridge Bioscience # GFH1–100) in 1 mL of PBS with 0.1% BSA. The required amount and type of cryogel microcarriers was added into each tube by creating a stock dispersion of the microcarriers in PBS and dividing it accordingly into each tube and kept at room temperature overnight to allow the growth factor to bind to cryogels. Tubes containing GDNF or BDNF solutions alone (without microcarriers) were also left at room temperature for the same time as a control for the possibility of protein degradation during the loading time. The next day, all tubes were centrifuged at 1300 rpm for 2 min and 900 μL of GDNF or BDNF loading solutions were removed (the remaining 100 μL at the bottom contained the loaded microcarriers) to be analyzed *via* ELISA to determine the concentration of protein remaining in the solution. Protein loaded = total protein added (control) - protein remaining.

To start the release study, the loaded microcarriers in the remaining 100 μL at the bottom of each tube were washed four times to remove any unbound protein by adding 900 μL release medium (PBS with 0.1% BSA to mimic competing protein binding which may occur *in vivo*) and centrifugation at 1300 rpm for 5 min. After washing, 900 μL fresh release medium was added and all tubes were incubated at 37 °C. Samples were collected at each time point by centrifugation at 1300 rpm for 2 min and removing 900 μL of the release medium and adding 900 μL fresh medium (the amount of GDNF or BDNF in the remaining 100 μL has been subtracted in the analysis). All samples and controls were stored at −20 °C until analysis of the GDNF or BDNF content *via* ELISA, which was performed according to the manufacturer's specification. An appropriate sample dilution was done for each sample to fit within the range of the assay. ELISA kits were purchased from R&D Systems, Human GDNF DuoSet ELISA #DY212, Human BDNF DuoSet ELISA # DY248 and DuoSet ELISA Ancillary Reagent Kit 2 #DY008.

2.5. Cytocompatibility analysis in vitro

Prior to performing the *in vivo* studies, *in vitro* cell culture studies were conducted to determine the cytocompatibility of PEGDA-SPA cryogels. This was assessed using alamarBlue® cell viability assay on cultures of human neuronal (SH-SY5Y) cell lines, human microglial (HMC3) cell lines, and rat primary neural cultures (embryonic day 14 (E14) ventral mesencephalon (VM)). Cells were cultured alone, with unloaded cryogels, with GDNF-loaded cryogels (using 80% SPA) or with BDNF-loaded cryogels (using 20% SPA), and the viability was assessed

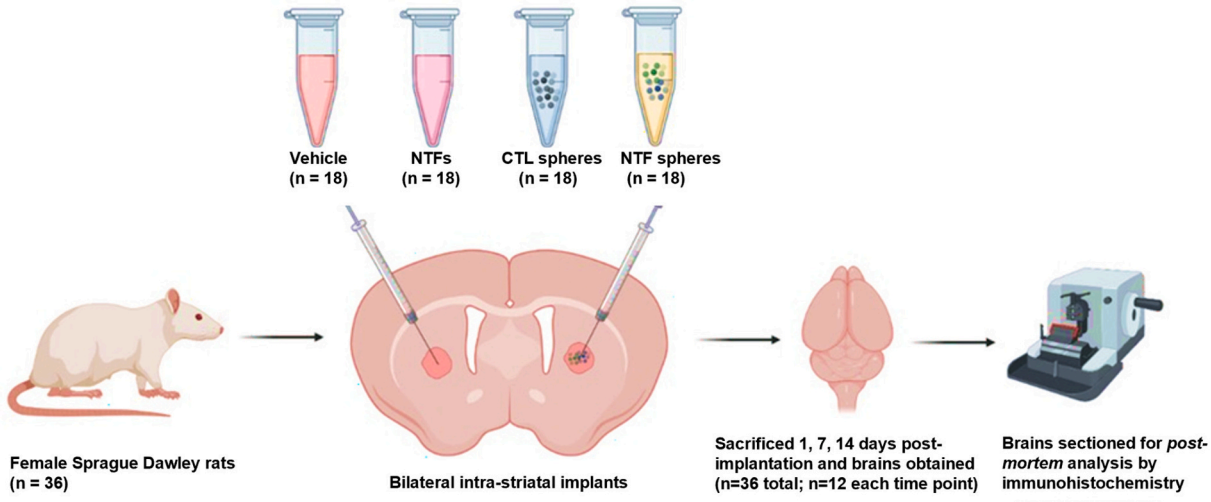

Fig. 2. Experimental design for biological studies *in vivo*. The *in vivo* biocompatibility of the cryogels, as well as their ability to deliver neurotrophins to the brain was then assessed by implanting them into the rat brain, and assessing neuroinflammatory and neurotrophin immunostaining at Days, 1, 7 and 14 after implantation, Created with BioRender.

up to Day 10. All *in vitro* analyses were carried out by an experimenter who was blind to the treatment of the cells.

2.5.1. Cell culture and viability analyses

SH-SY5Y cells were cultured in 1:1 Dulbecco's modified Eagle's medium/Nutrient mixture F-12 Ham containing 10% FCS, 1% penicillin/streptomycin and 1% L-glutamine at 37 °C with 5% CO_2. HMC3 cells were cultured in Dulbecco's modified Eagle's medium – high glucose containing 10% FCS and 1% penicillin/streptomycin at 37 °C with 5% CO_2. VM cells were plated and cultured in Dulbecco's modified Eagle's medium/ Nutrient mixture F-12 Ham, 0.6% D-glucose, 1% L-glutamine, 1% FCS and 2% B27 at 37 °C with 5% CO_2. SH-SY5Y and HMC3 were seeded at a density of 30,000 cells per well of a 24 well-plate while E14 VM cells were seeded on poly-D-lysine (Sigma) coated 24 well plates, at a density of 100,000 cells per well. To determine the cytocompatibility of the cryogels, 80% SPA cryogels were first loaded with GDNF (500 ng/0.01 mg cryogels) while 20% SPA cryogels were loaded with BDNF (500 ng/0.01 mg cryogels) as described above. 0.01 mg of unloaded cryogels, GDNF-loaded cryogels or BDNF-loaded cryogels were then added to the wells 30 min prior to seeding the cells, and viability was assessed using the alamarBlue® assay as previously described [29,30] at Days 2, 4, 7 and 10 (SH-SY5Y cultures), Days 1, 2 and 4 (HMC3 cultures) or Days 1, 2, 3 and 4 (VM cultures) post-plating. All data points represent 3 biological replicates per pretreatment group (with 3 technical replicates).

2.5.2. Immunocytochemistry

To complement the quantitative viability assays, qualitative visualization of the primary neural cultures was also completed at 5 days post-plating in the presence or absence of loaded or neurotrophin-loaded cryogels using pan neuronal immunocytochemistry (beta-III tubulin) counterstained with nuclear staining (DAPI) as previously described [20,31]. In brief, VM cultures were fixed with 4% paraformaldehyde for 30 min, followed by three washes in tris-buffered saline (TBS) with 0.2% triton-X-100 for permeabilization. Cultures were then incubated in blocking serum (5% bovine serum albumin (BSA) in TBS with 0.2% triton-X-100) for 1 h at room temperature, before being subsequently incubated with primary antibody (Mouse anti-beta III tubulin, 1:200, Millipore) diluted with 1% BSA in TBS with 0.2% triton-X-100 at room temperature overnight. Following 3 × 10 min washes with TBS, cultures were incubated in rabbit anti-mouse AF 488 conjugated secondary antibody (1:1000, Biosciences) in 1% bovine serum albumin in TBS, at room temperature for 3 h in darkness. Cultures were then counterstained with DAPI (1 μg/mL in TBS, Sigma) for 5 min. Following 3 × 10 min washes in TBS, cultures were stored in 0.1% TBS azide at 4 °C until image capture on an EVOS M7000 microscope (Invitrogen / Thermo Fisher Scientific).

2.6. In vivo analysis of biocompatibility and local growth factor delivery

An *in vivo* study was then undertaken to determine the biocompatibility of the cryogels after implantation into the brain, as well as their ability to deliver neurotrophins to, and retain neurotrophins in, the striatum (Fig. 2). Female Sprague Dawley rats ($n = 36$) were randomly assigned to receive bilateral intra-striatal implants of either vehicle, unloaded cryogels, neurotrophins-alone or neurotrophin-loaded (GDNF & BDNF) cryogels. Rats were sacrificed at Days 1, 7 and 14 post-implantations ($n = 6$ per group per time point) for *post-mortem* immunohistochemical analysis of biocompatibility (microgliotic and astrocytic response to the implant), as well as GDNF and BDNF delivered to/retained at the implant site and released into the peri-implant region. All *in vivo* analyses were carried out by an experimenter who was blind to the treatment of the animals.

2.6.1. Animals

All experiments involving the use of animals for procedures and cell preparations were performed in compliance with the European Union Directive 2010/63/EU and Irish S·I No. 543 of 2012, were completed under Project and Individual Authorisation by the Irish Health Products Regulatory Authority and were approved by the Animal Care and Research Ethics Committee at the University of Galway. For primary neural cultures, time-mated female Sprague-Dawley rats ($n = 6$) were sourced from Janvier Labs, France, anaesthetized using isoflurane gaseous anesthesia (5% in O_2) and decapitated. The uterine horns were then obtained *via* laparotomy, the VM micro-dissected from each E14 embryo, and singe cell suspensions for cell culture prepared as previously described [32]. For the *in vivo* study, female Sprague Dawley rats ($n = 36$; weighing 250–275 g on arrival) were sourced from Janvier Labs, France. Animals were housed in groups of three per cage, on a 12:12 h light/dark cycle, at 19–23 °C, with relative humidity levels maintained between 40% and 70%. For the duration of the experiment, animals were allowed food and water *ad libitum*.

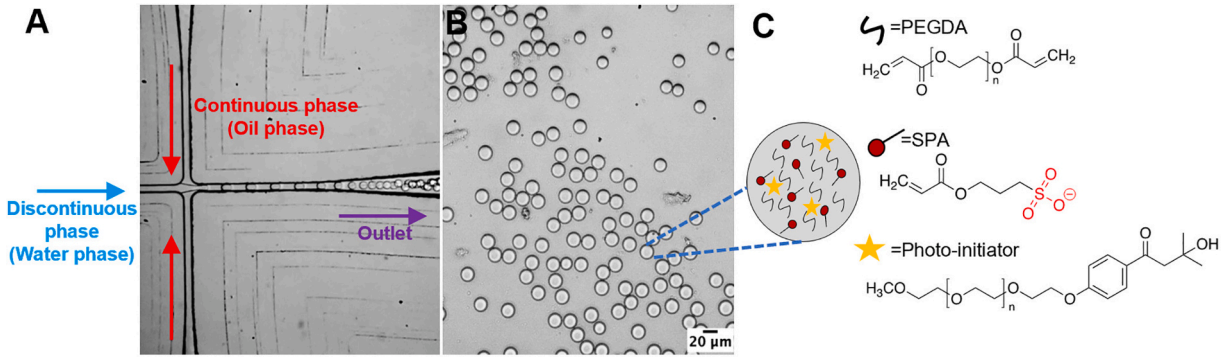

Fig. 3. Droplet formation using microfluidic device with flow focusing cross-junction for W/O emulsion formation. (A) Microscopic image of cross-junction site of the microfluidic device (Fluidic 947, T junction size = 20 μm) showing the first inlet (blue) for discontinuous phase (monomer precursor solution), the second inlet (red) for the continuous phase (oil and surfactant), and the outlet (violet). (B) Monodisperse droplets with an average diameter of 20 μm were produced. (C) Chemical structures of prepolymer solution components. (For interpretation of the references to colour in this figure legend, the reader is referred to the web version of this article.)

2.6.2. Stereotaxic surgery

Female Sprague Dawley rats (n = 36) were randomly assigned to receive bilateral intra-striatal implants of either vehicle (Dulbecco's modified Eagle's medium/ Nutrient mixture F-12 Ham, 0.6% D-glucose, 1% L-glutamine, 1% FCS and 2% B27), unloaded cryogels (0.01 mg each of 80% SPA and 20% SPA per transplant), neurotrophins-alone (500 ng each of GDNF & BDNF per transplant), or neurotrophin-loaded cryogels. All surgeries were performed under isoflurane anesthesia (5% in O_2 for induction and 2% in O_2 for maintenance) in a stereotaxic frame with the nose bar set at −2.3 as previously described [20,33]. The striatum was infused at coordinates Antero-Posterior (AP) = 0.0, Medial-Lateral (ML) ±3.7 (from bregma) and Dorsal-Ventral (DV) −5.0 below dura. Infusions were completed at a total volume of 6 μL at a rate of 1 μL/min with a further 2 min allowed for diffusion. Animals were then sacrificed at Days 1, 7 and 14 by terminal anesthesia (50 mg/kg pentobarbital intraperitoneal (i.p.)) and transcardial perfusion with 100 mL heparinized saline followed by 150 mL of 4% PFA. Brains were rapidly removed and placed in 4% PFA overnight before being cryoprotected in 25% sucrose solution.

2.6.3. Immunohistochemistry

Serial coronal sections (30 μm) were cut using a freezing stage sledge microtome (Bright, Cambridgeshire, UK) and free-floating immunohistochemistry for microgliosis (cd11b), astrocytosis (glial fibrillary acidic protein (GFAP)), GDNF and BDNF was performed as previously described [33,34]. In short, endogenous peroxidase activity was quenched using a solution of 3% hydrogen peroxidase and 10% methanol in distilled water. Non-specific binding was blocked using 3% normal horse serum (cd11b, GDNF, BDNF,) or normal goat serum (GFAP) in TBS with 0.2% Triton-X-100. Primary antibody (Mouse anti-cd11b, 1:400, Millipore; Rabbit anti-GFAP, 1:2000, Dako; Mouse anti-GDNF, 1:200, R&D Systems; Mouse anti-BDNF, 1:200, R&D Systems) was diluted in TBS with 0.2% triton-X-100, added to sections and incubated at room temperature overnight. Sections were incubated in secondary antibody (Horse anti-mouse, 1:200, Vector; Goat anti-rabbit, 1:200, Jackson ImmunoResearch) for 3 h at room temperature. A

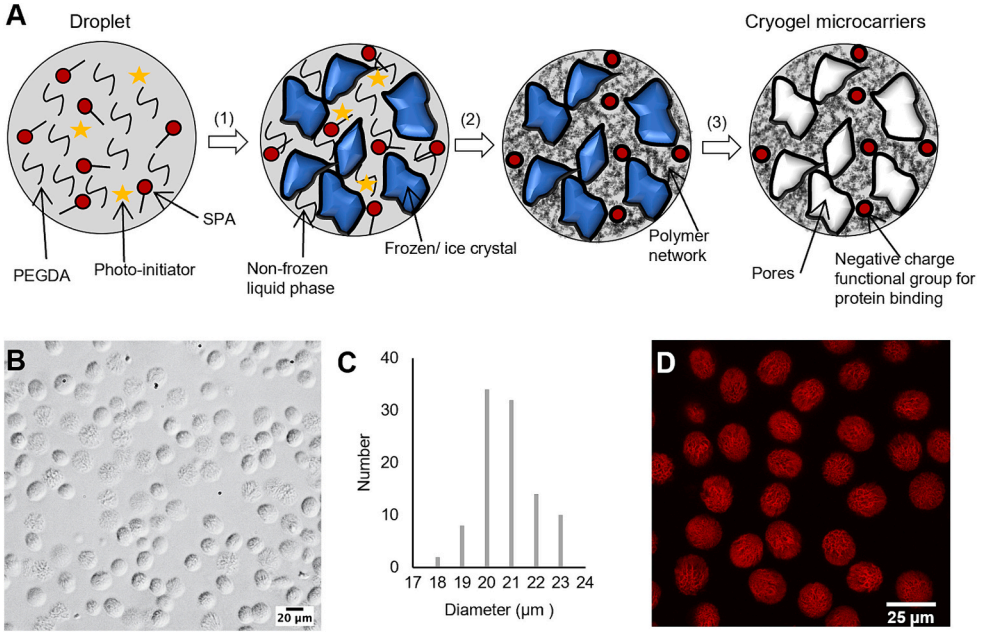

Fig. 4. The emulsion templating results in near-monodisperse cryogel microcarrier formation. (A) An overview of the cryogelation technique to create microporous structure of PEGDA-co-SPA cryogel microcarriers. 1- Freezing induced ice crystal formation. 2- UV light-initiated photo-polymerization within the non-frozen liquid phase formed the polymer network. 3- Thawing reveals the porous structure. (B) Small and monodisperse cryogels were developed (C) with a narrow size distribution of 21.2 ± 1.1, (n = 100 from 95% SPA cryogels). (D) Confocal fluorescence microscopy image showing iFluor™ 647 labeled, hydrated cryogel microcarriers.

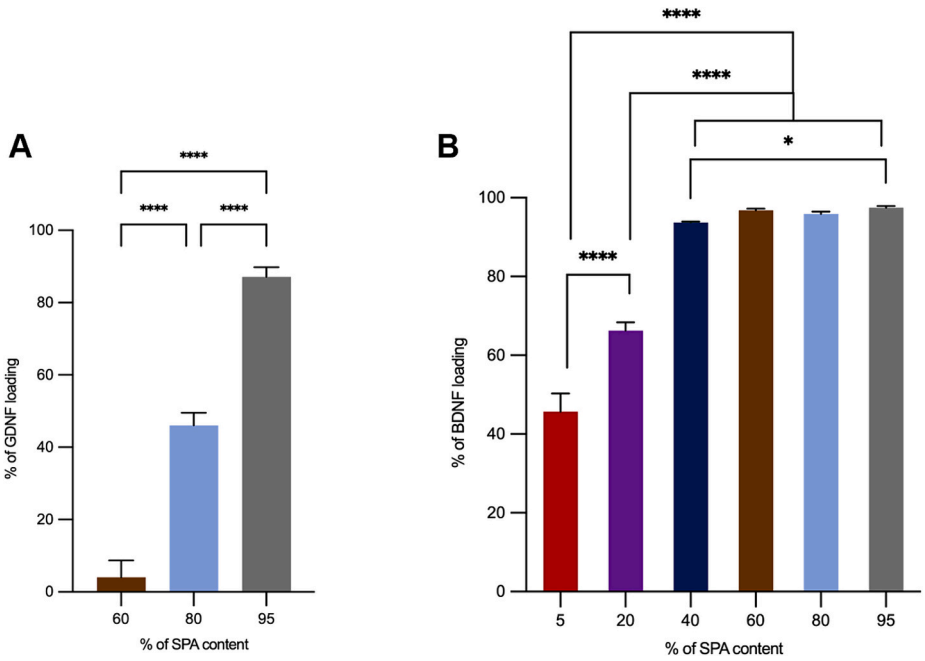

Fig. 5. Protein loading into cryogel microcarriers is dependent on SPA content. 100 ng of GDNF (A) or BDNF (B) were added to the cryogel microcarriers. ELISA analysis of the supernatants the following day showed no GDNF loading to 60% SPA cryogels while 95% cryogels showed the highest loading, whereas all types of cryogels were able to load BDNF. $n = 3$ for all experiments and error bars represent ± standard deviation $^{*}P < 0.05$ and $^{****}P < 0.0001$ *via* one-way ANOVA.

streptavidin-biotin-horseradish peroxidase solution (Vector, UK) was subsequently added to sections and allowed to incubate for 2 h. The development of staining was carried out using a 0.5% solution of diaminobenzidine tetra hydrochloride (DAB, Sigma) in TBS containing 0.3 μL/mL of hydrogen peroxide. Sections were mounted onto gelatin-coated slides, dehydrated in a series of ascending alcohols, cleared in xylene and finally coverslipped using DPX mountant (Sigma) for DAB-stained sections.

2.6.4. Image analysis

The optical density of microgliosis and astrocytosis, as well as GDNF and BDNF immunostaining, within and immediately adjacent to the implant site, were measured from a 1:6 series of sections. Photomicrographs of three sections along the rostro-caudal axis of the striatum were analyzed for mean grey values using ImageJ software and converted into optical density (arbitrary units) by applying the following formula: OD = log10 (255/mean grey value). Implant volume, and volume of neurotrophin staining, were also measured using cross-sectional areas from a 1:6 series of sections, and Cavalieri's Principle was applied to determine volume as previously described [35]. Sphere sizes *in vivo* were also measured in neurotrophin immunostained sections (5 cryogels randomly measured per rat).

2.7. Statistical analysis

Protein loading data are expressed as mean ± standard deviation and analyzed using one-way analysis of variance (ANOVA). Cytocompatibility and biological studies data are expressed as mean ± standard error of the mean and analyzed using 2-way or 2-way repeated measures ANOVA as appropriate. Throughout the results text, the main effects from the initial ANOVA are cited in the body of the results, while the results of the *post-hoc* analyses are shown on the corresponding figure and explained in the figure legend.

3. Results

3.1. Synthesis of porous and monodisperse cryogel microcarriers

Monodisperse emulsion droplets were produced using the Fluidic 947 microfluidic device (Fig. 3A and B) to serve as templates for cryogel production. The droplets contained the monomer (SPA), crosslinker (PEGDA), and photo-initiator (PEG-Irgacure 2959) (Fig. 3C). Small photoinitiators like Irgacure 2959 tend to diffuse outside the droplets into the oil phase due to the hydrophobicity of the generated radicals [27]. Therefore, PEGylation of Irgacure 2959 was performed to improve the water solubility to retain the free radicals inside the water droplets. This consequently improves the polymerization efficiency of the monomers ensuring complete crosslinking of the polymer network.

During the cryogelation process (Fig. 4A), each droplet transformed into a cryogel of the same size and shape. As shown in in Fig. 4B and C, small and monodisperse cryogels with a narrow size distribution of 21.2 ± 1.1 μm were formed. To analyze how the SPA inclusion affects the protein loading/release properties, cryogel microcarriers were fabricated that contained different SPA contents (5%, 20%, 40%, 60%, 80% and 95% SPA cryogels). The cryogelation process forms the polymer network *via* UV light induced photopolymerization of PEGDA and SPA within the non-frozen liquid phase. The reaction steps for photopolymerization are explained in Fig. S1. FTIR spectroscopy analysis of all SPA cryogels was performed in comparison to the pure monomers as shown in Fig. S2. The results provide evidence of complete covalent bonding within the cryogel network and thus no free vinyl groups remain in the structure. Confocal laser microscopy showed the monodisperse and microporous structure of iFluor™ 647 labeled cryogel microcarriers (Fig. 4D).

3.2. Growth factor loading and release analysis in vitro

3.2.1. Protein loading into cryogel microcarriers is dependent on SPA content

100 ng of the protein without cryogels was used to test the protein stability in PBS with 0.1% BSA at different conditions. The positive

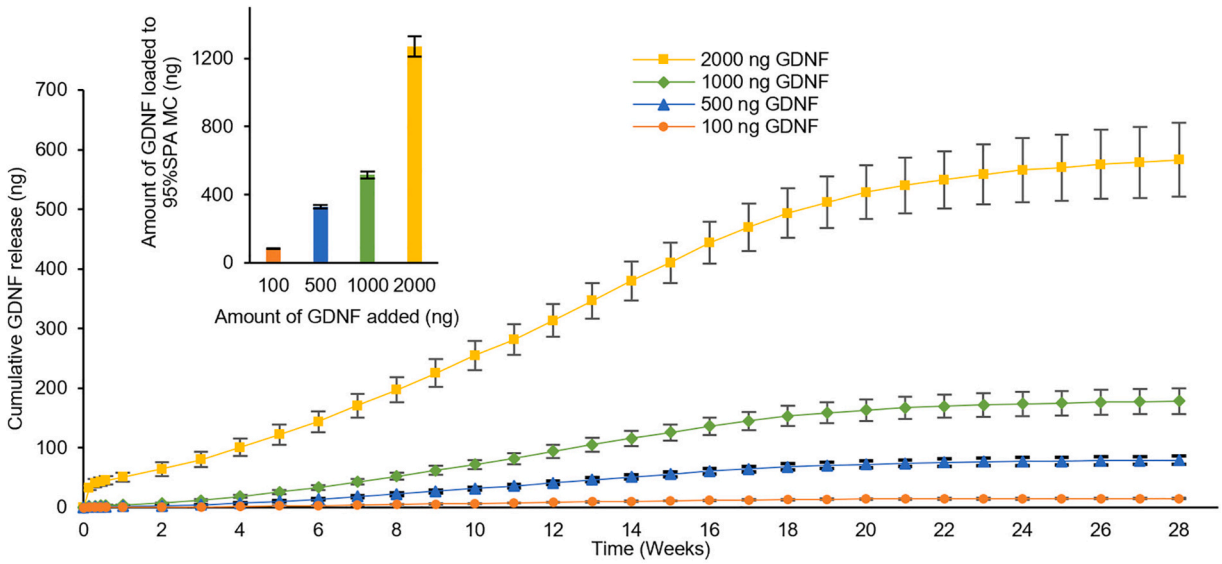

Fig. 6. GDNF loaded to 95% SPA cryogel microcarriers is released slowly for seven months. Different amounts of GDNF (100, 500, 1000, 2000 ng) were added to 0.01 mg cryogels and the total amount loaded for each amount is shown in the inset figure. Cumulative GDNF release (ng) over 7 months in PBS + 0.1% BSA was measured at each time point *via* ELISA. For 2000 ng GDNF, around 46% of loaded GDNF was released by week 28 (longest time tested), $n = 3$ for all experiments and error bars represent ± standard deviation.

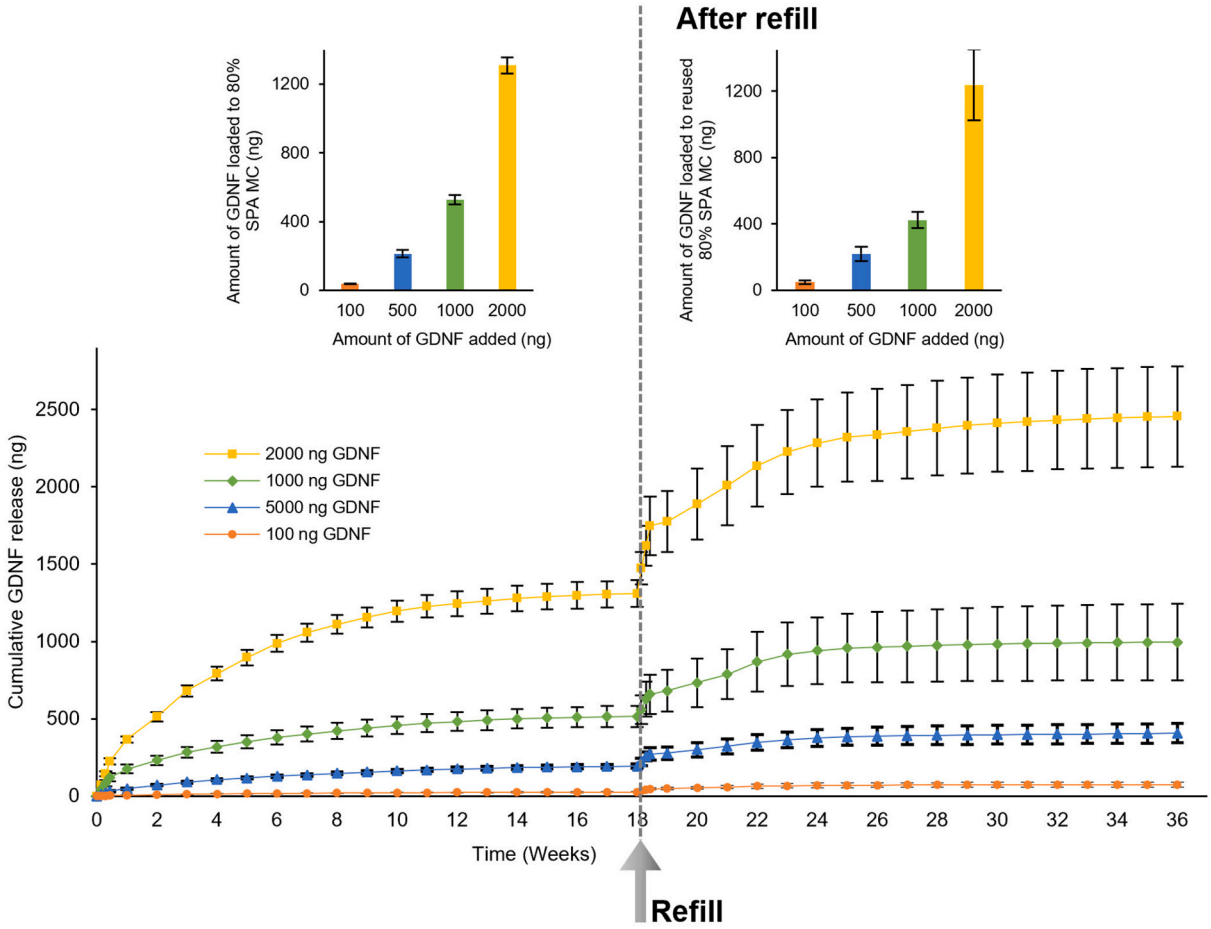

Fig. 7. 80% SPA cryogel microcarriers can release GDNF over 4 months and can be refilled. Different amounts of GDNF (100, 500, 1000, 2000 ng) were added to 0.01 mg cryogels (amount loaded in inset graph) and cumulative GDNF release (ng) was analyzed over 9 months. When all the GDNF had been released at week 18 the 80% SPA cryogel microcarriers were washed 4× with PBS and reloaded (right hand inset graph) with different amounts of GDNF (100, 500, 1000, 2000 ng) showing a similar loading amount and release profile as in the first time. $n = 3$ for all experiments and error bars represent ± standard deviation.

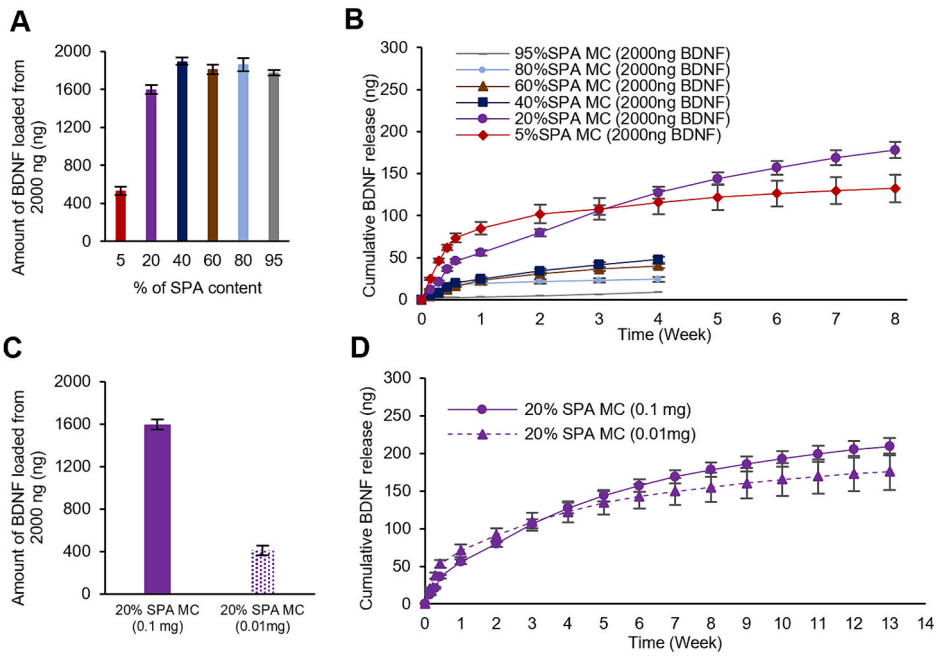

Fig. 8. BDNF loading and release experiment using 5%, 20%, 40%, 60%, 80% and 95% SPA MC. (A) 2000 ng BDNF was added to 0.1 mg cryogel microcarriers showing a high loading, >1600 ng for all except 5% SPA cryogels, which showed a substantial decline to approximately only 500 ng. (B) Analysis of cumulative BDNF release over one month showed that decreasing the negative charge increased the release of protein. (C) 2000 ng BDNF was loaded to 0.1 mg *Vs.* 0.01 mg of 20% SPA MC and the latter showed less BDNF loading, but (D) a similar release profile. $n = 3$ for all experiments and error bars represent ± standard deviation.

control was 100 ng of the protein prepared and measured on the same day of the experiment. The detected amount of both 100 ng of GDNF and BDNF remained the same after one day at room temperature, one day at 37 °C or one week at 37 °C (Fig. S3). Cryogel microcarriers with 5%, 20%, 40%, 60%, 80% and 95% SPA content were prepared to analyze the effect of SPA amount on the protein loading properties of the microcarriers. All types of cryogels had the same size and shape (Fig. S4). 60% SPA cryogels were unable to load 100 ng of GDNF, but 80% SPA and 95% SPA cryogels loaded around 45% and 85% of the GDNF respectively (Fig. 5A). On the other hand, almost all the 100 ng of BDNF was loaded to cryogels with an SPA content of 40% SPA or higher (Fig. 5B).

3.2.2. *GDNF release characteristics from 95% SPA cryogels and exploration of enhanced release with 80% SPA cryogels in PBS + 0.1% BSA*

Since 95% SPA cryogels (with the highest negative charge) showed a high loading capacity, we decided to start using them for the first loading/release analysis. Initially, we aimed to determine the minimum amount of cryogels that can effectively load GDNF to maximize loading efficiency and minimize dead space in the brain during *in vivo* analyses. Thereby, GDNF was added to three different cryogel masses 0.5, 0.1 and 0.01 mg of 95% SPA cryogels. Fig. S5 shows that even the lowest mass of 0.01 mg was still able to load different amounts of GDNF. Therefore, 0.01 mg of cryogels were used for GDNF loading/release studies as well as for later *in vivo* biological studies. After that, different amounts of GDNF were added to 0.01 mg of 95% SPA cryogels and a sample was taken every week to measure the amount of GDNF released. The results demonstrated that GDNF was released very slowly over a period of seven months without an initial burst release (Fig. 6). For example, 2000 ng GDNF-loaded cryogel released 583 ng (approximately 50% of the loaded amount (1270 ng)).

The release profile of GDNF from 95% SPA cryogels displayed a notably slow and sustained trend. To increase the release rate for shorter-term applications, our attention turned towards the utilization of 80% SPA cryogels that are characterized by less sulfonate groups. In a similar way, varying quantities of GDNF were added to 80% SPA cryogels and a sample was taken on a weekly basis to measure the amount of GDNF released. Interestingly, GDNF exhibited a gradual and sustained pattern of release over four months until all was released (Fig. 7).

Having achieved both medium- and long-term release of GDNF, we wanted to assess the potential to refill these cryogels, which would unlock almost limitless release profiles. The same 80% SPA cryogels were washed and reloaded with the same amount of GDNF protein. The cryogels were able to rebind to GDNF and release it again. Remarkably, both the refill and re-release profiles closely matched that of the initial loading/release study for all four loading quantities thus allowing predictable release refilled systems (Fig. 7).

3.2.3. *BDNF loading and release is highly dependent on the SPA content in the cryogels*

The experimental outcomes of BDNF loading and release using 0.1 mg of 95%, 80%, 60%, 40%, 20% and 5% SPA cryogels with different amounts of BDNF are shown in Fig. S6. All loading amounts from 2000 ng of BDNF were >1600 ng apart from 5% SPA cryogels, which showed a substantial decline to approximately only 500 ng (Fig. 8A). The release of BDNF was measured for one month, for 95%, 80%, 60% and 40% SPA cryogels and two months for 20% and 5% SPA cryogels (Fig. 8B). In contrast to GDNF, BDNF was not released from 95% SPA cryogels. Besides, the release from 80%, 60% and 40% was very slow and almost none was released over one month. However, decreasing the negative charge to 20% or 5% improved the BDNF release rate. It appears that the release depends on the charge density of the cryogels, and less negative charge caused less electrostatic interaction with the protein hence increasing the release rate. We speculate that there may be a threshold charge density for strong retention of proteins (*i.e.* at about 20% SPA in the case of BDNF). This might explain why cryogels with 40 and 60% SPA content show similar release profiles, whist 20% SPA (and lower) exhibits a significant increase in the release rate.

Specifically, the release of BDNF from 5% SPA cryogels was higher (85 ng) compared to 20% SPA cryogels (50 ng) after one week. After that, minimal release was observed with 5% SPA cryogels while the release from the 20% SPA cryogels was sustained and continuous, reaching around 180 ng over two months. This sustained release pattern prompted the selection of 20% SPA cryogels to be used for the

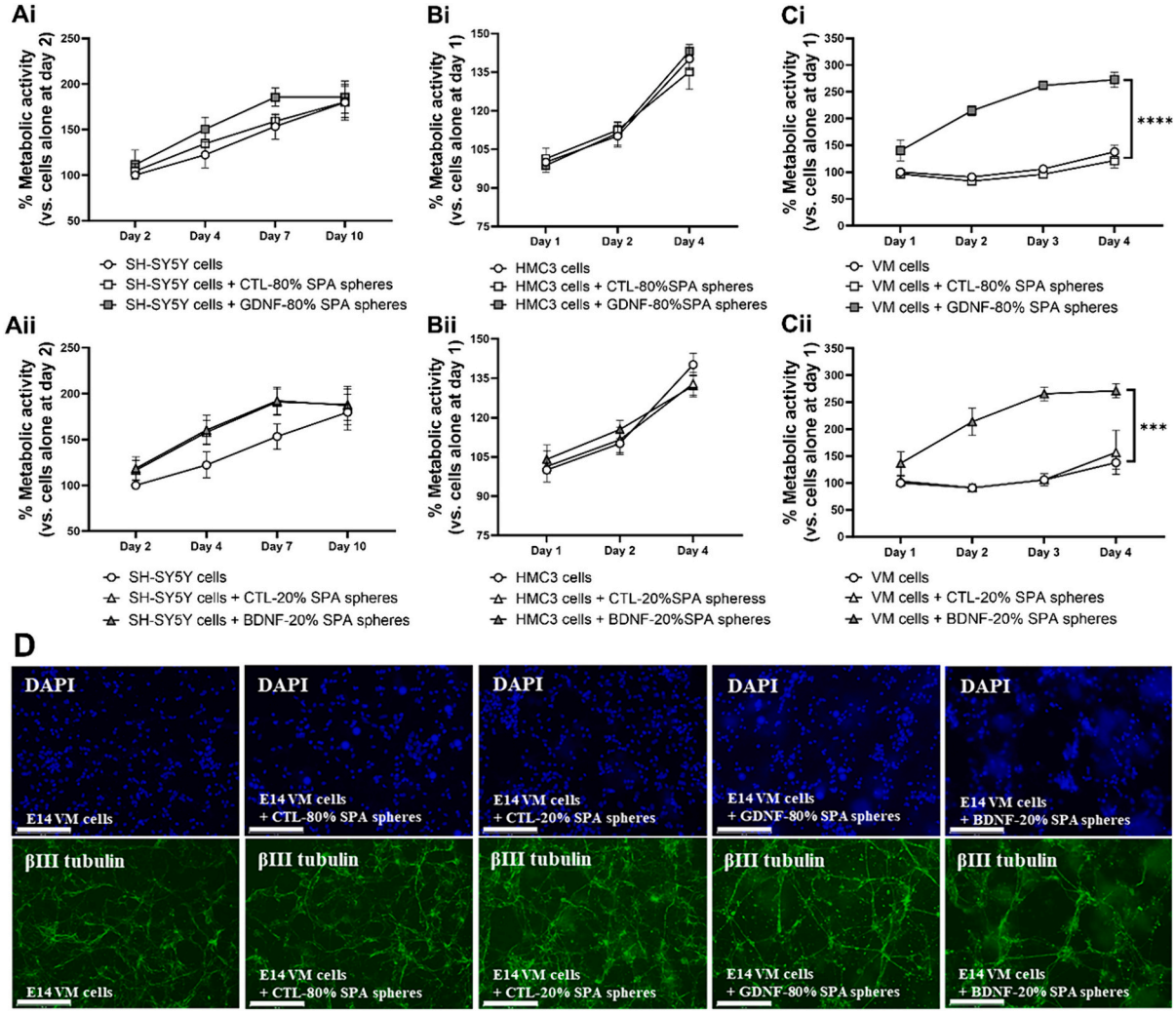

Fig. 9. Cytocompatibility of PEGDA-SPA cryogels with human neuronal cells, human microglial cells, and rat primary neural (E14 VM) cultures. SH-SY5Y cells, HMC3 cells and E14 VM cultures were incubated with 80% SPA cryogels empty (CTL) or loaded with 500 ng GDNF (Ai, Bi, Ci) or 20% SPA cryogels unloaded or loaded with 500 ng BDNF (Aii, Bii, Cii). Viability analyses confirmed the cytocompatibility of the cryogels and demonstrated a pronounced trophic effect on the primary neural cultures. Visualization of the VM cultures at Day 5 (using immunofluorescence for beta-III tubulin) (D) confirmed a healthy neuronal population in the presence of the cryogels. Scale bar represents 150 μm. Data are represented as mean ± SEM of $n = 3$ biological replicates. ****$P < 0.0001$, ***$P < 0.001$ by two-way repeated measures ANOVA.

subsequent *in vivo* investigations. To proceed *in vivo*, it was crucial to establish that the lowest mass, 0.01 mg of 20% SPA cryogel is capable of loading BDNF. The results showed a reduction in BDNF loading by 4-fold from 1600 ng to 400 ng for 0.1 mg and 0.01 mg respectively. However, it is notable that the release profile remained almost unaltered throughout the extended observation period of three months as shown in (Fig. 8C).

3.3. PEGDA-SPA cryogels are cytocompatible with human neuronal cells, human microglial cells and rat primary neural cultures

To confirm their cytocompatibility, 80% SPA microcarriers, empty (control) or loaded with 500 ng GDNF, or 20% SPA microcarriers, empty or loaded with 500 ng BDNF, were incubated with human neuronal SH-SY5Y cells, human microglial HMC3 or rat E14 VM cultures and cell viability was measured over time (Fig. 9). The cryogels were fully cytocompatible with human neurons and human microglia with no difference in viability over time relative to cells incubated alone (Fig. 9 Ai; Group x Time, $F_{(6, 18)} = 0.690$, $P > 0.05$; Aii; Group x Time, $F_{(6, 18)} = 1.581$, $P > 0.05$; Bi; Group x Time, $F_{(4, 12)} = 0.603$, $P > 0.05$; Bii; Group x Time, $F_{(4, 12)} = 0.684$, $P > 0.05$). Strikingly, with the primary neural cultures, while the non-loaded control microcarriers had no effect on the viability, the neurotrophin-loaded microcarriers dramatically increased the culture viability of the cultures over time suggesting a functional trophic effect (Fig. 9 **Ci**; Group x Time, $F_{(6, 18)} = 9.42$, $P < 0.0001$; Cii; Group x Time, $F_{(6, 18)} = 8.46$, $P < 0.001$). Visualization of the VM cultures at Day 5 (using immunofluorescence for beta-III tubulin counterstained with DAPI nuclear stain, Fig. 9D) confirmed the cytocompatibility of the microcarriers.

3.4. Biocompatibility of PEGDA-SPA cryogels in the rat brain

After determining the *in vitro* cytocompatibility of PEGDA-SPA cryogels, we aimed to study their *in vivo* biocompatibility in the brain. Rats were given intra-striatal implants of either vehicle, non-loaded (empty) cryogels (0.01 mg each of 80% SPA and 20% SPA per transplant), neurotrophins-alone (500 ng each of GDNF & BDNF per transplant), or neurotrophin-loaded cryogels and sacrificed at Days 1, 7 and 14 post-implantation. Biocompatibility was assessed *via* analysis of the microgliotic and astrocytic response within, and surrounding, the implant site. As expected, the stereotaxic procedure itself, even with administration of vehicle alone, induced pronounced microgliotic (Fig. 10) and astrocytic (Fig. 11) responses in the striatum. Furthermore, at the earliest

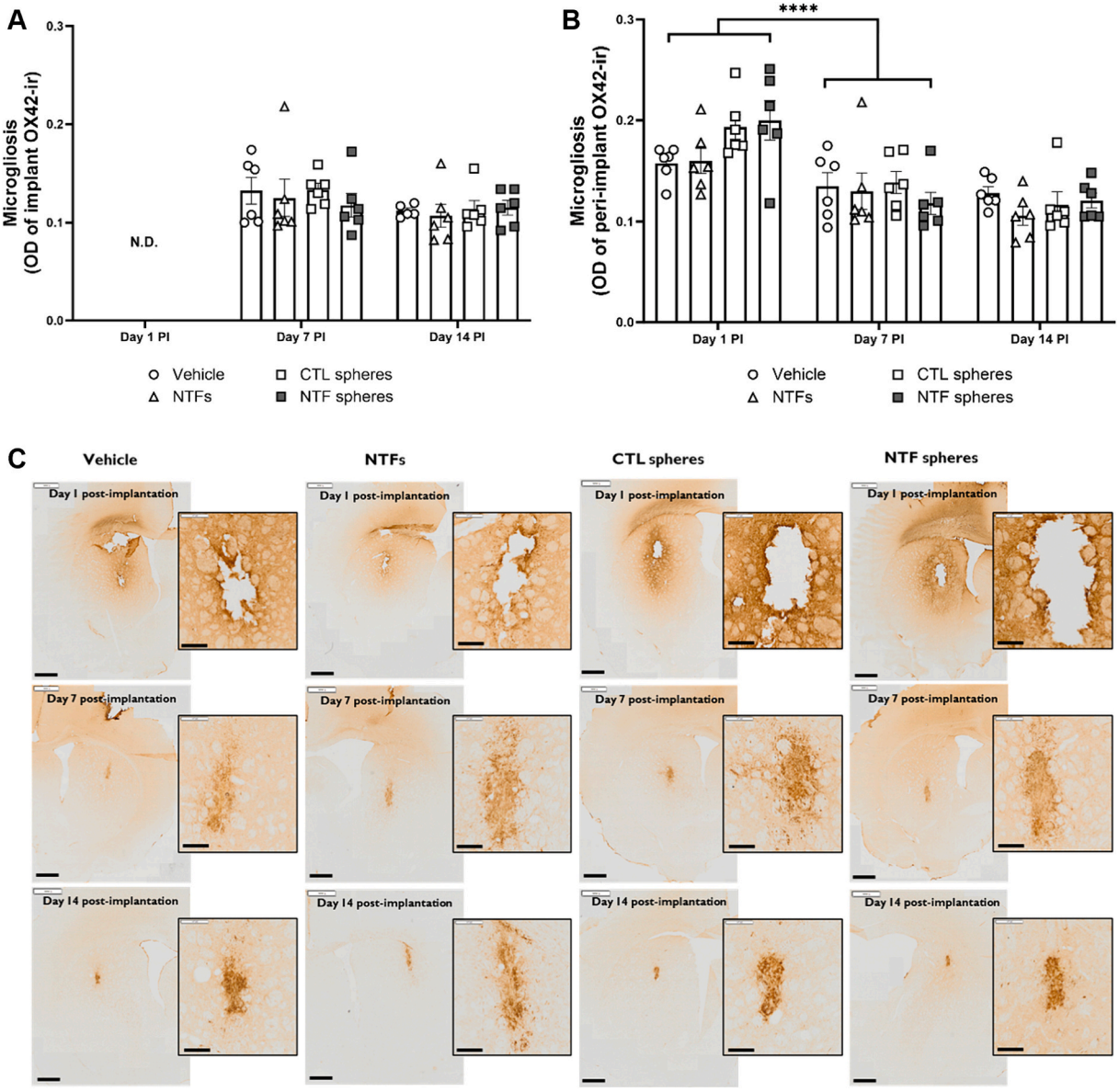

Fig. 10. Cryogels elicit no additional microglial response in the rat brain compared to a vehicle alone injection. The biocompatibility of the implanted cryogels was assessed by measuring the optical density of striatal microgliosis at the implant site at Days 7 and 14 post-implantation (A), and in the peri-implant region at Days 1, 7 and 14 post-implantation (B). The cryogels, either unloaded or loaded with neurotrophins, did not induce any greater microgliotic response either within (A, C), or surrounding (B, C), the implant site relative to that caused by administration of vehicle alone. Scale bar represents 1 mm and 200 μm (inset). Data are represented as mean ± SEM of $n = 6$ rats. ****$P < 0.0001$ by two-way ANOVA. N.D. = not done.

time-point (Day 1 after implantation) there was visible damage at the injection site in all groups meaning that neuroinflammatory responses at the site of injection could not be determined at that time-point. However, this damage had resolved by Day 7 post-implantation so the effect of the cryogels, relative to vehicle administration, could be assessed at the later time-points, both within and surrounding the implant site.

In terms of inflammatory responses to the cryogels within the injection site itself, there was no difference in the density of either microgliosis (Fig. 10A: Group x Time, $F_{(3,\ 39)} = 0.28$, $P > 0.05$) or astrocytosis (Fig. 11A: Group x Time, $F_{(3,\ 37)} = 0.59$, $P > 0.05$) between groups at Day 7 or Day 14, demonstrating that the cryogels, either unloaded or loaded with neurotrophins, did not induce any inflammatory reaction over and above that caused by injection of vehicle alone. Similarly, when assessing the inflammatory response surrounding the injection site, there was no difference in the density of either microgliosis (Fig. 10B: Group x Time, $F_{(6,\ 60)} = 1.58$, $P > 0.05$) or astrocytosis (Fig. 11B: Group x Time, $F_{(6,\ 60)} = 1.44$, $P > 0.05$) between groups at Day 1, Day 7 or Day 14, again demonstrating the biocompatibility of the cryogels *in vivo* in the rat brain. Interestingly, the pronounced microglial reaction surrounding the site of injection had largely subsided by Day 7 in all groups (Fig. 10B: Time, $F_{(2,\ 60)} = 26.62$, $P < 0.0001$) whereas the astrocyte density increased in the striatum in all groups (Fig. 11B: Time, $F_{(2,\ 60)} = 46.99$, $P < 0.0001$).

3.5. *PEGDA-SPA cryogels as vehicles for delivery of neurotrophins to the brain*

After confirming the *in vivo* biocompatibility of the PEGDA-SPA cryogels in the brain, we went on to assess their ability to deliver neurotrophins to, and retain neurotrophins within, the brain. Neurotrophin delivery and retention were assessed *via* analysis of GDNF and BDNF immunostaining within, and surrounding, the implant site. As was the

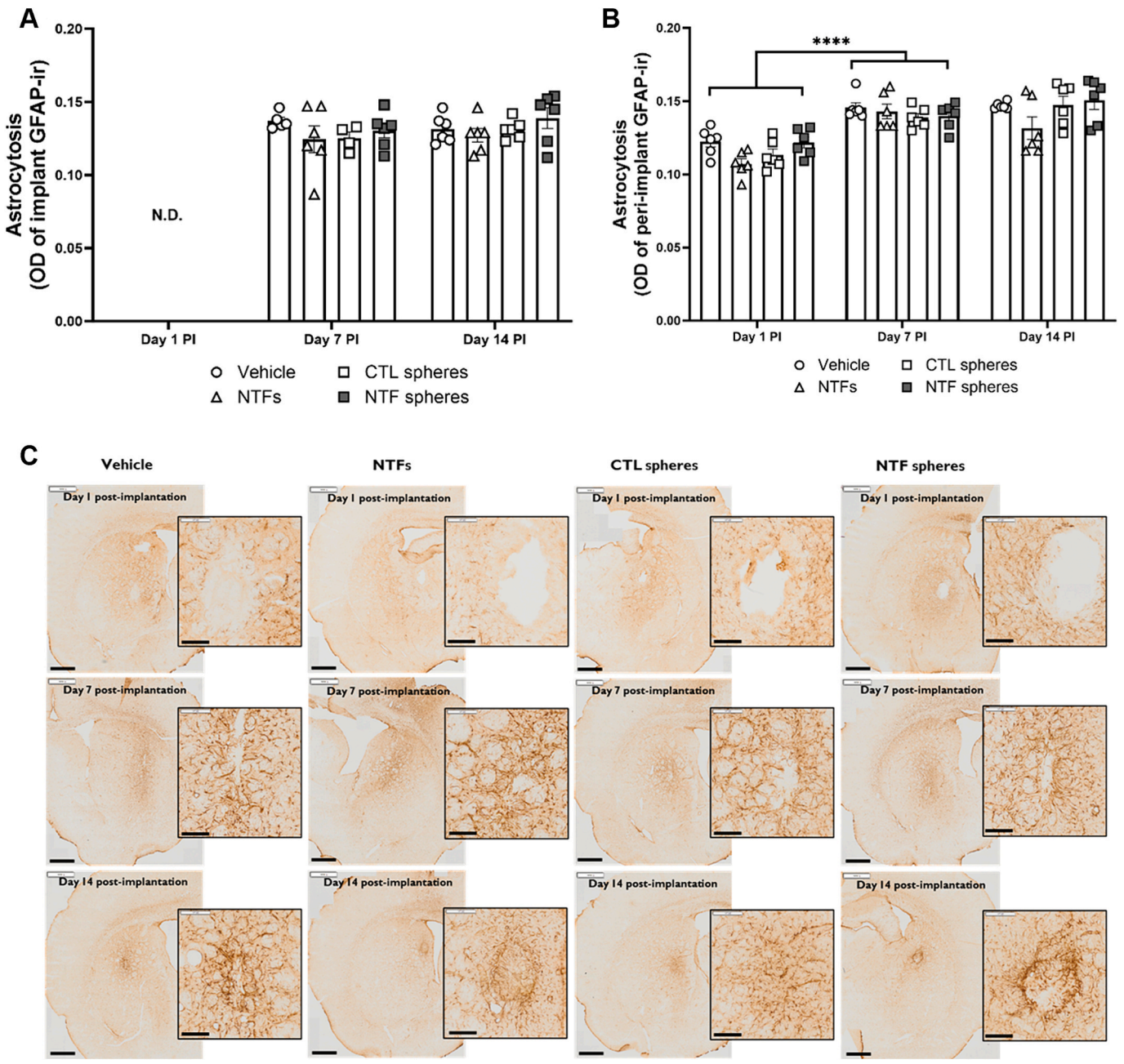

Fig. 11. Cryogels elicit no additional astrocytic response in the rat brain compared to a vehicle alone injection. The biocompatibility of the implanted cryogels was assessed by measuring the optical density of striatal astrogliosis at the implant site at Days 7 and 14 post-implantation (A), and in the peri-implant region at Days 1, 7 and 14 post-implantation (B). The cryogels, either unloaded or loaded with neurotrophins, did not induce any greater astrocytic response either within (A, C), or surrounding (B, C), the implant site relative to that caused by administration of vehicle alone. Scale bar represents 1 mm and 200 μm (inset). Data are represented as mean ± SEM of n = 6 rats. ****$P < 0.0001$ by two-way ANOVA. N.D. = not done.

case for the biocompatibility analysis above, the damage to the striatum caused by the stereotaxic injection itself, meant that GDNF and BDNF immunostaining within the injection site could not be quantified at Day 1 post-implantation. As there was no GDNF or BDNF staining evident in the peri-implant region at this early time-point (not shown), only the Day 7 and Day 14 time-points were analyzed.

In terms of GDNF delivery, when the GDNF was injected into the striatum alone as a bolus, there was no residual staining visible by Day 7 after administration (Fig. 12). In contrast, when the neurotrophin was loaded into PEGDA-SPA cryogels, the GDNF-loaded cryogels were clearly visible in the striatum at both Days 7 and 14 after implantation (Fig. 12A; Group, $F_{(3,\ 37)} = 83.93$, $P < 0.0001$) confirming successful delivery to, and retention of, GDNF in the striatum. Similarly, for BDNF, no staining was visible in the striatum by Day 7 when the neurotrophin was injected alone as a protein bolus (Fig. 13), but pronounced staining was visible at both later time-points when it was loaded onto cryogels (Fig. 13A; Group, $F_{(3,\ 37)} = 51.49$, $P < 0.0001$).

To determine release of neurotrophins from the cryogels in the brain, we analyzed the density of GDNF and BDNF surrounding the implant site. By Day 7 after implantation, there was a clearly visible region of GDNF staining surrounding the implant site in the brains implanted with GDNF-loaded cryogels confirming release of the neurotrophin into the peri-implant region (Fig. 12B; Group, $F_{(3,\ 38)} = 12.66$, $P < 0.0001$). By Day 14 after implantation, there was also a clearly visible region of BDNF staining surrounding the implant site in some of the brains implanted with BDNF-loaded cryogels but this was more variable

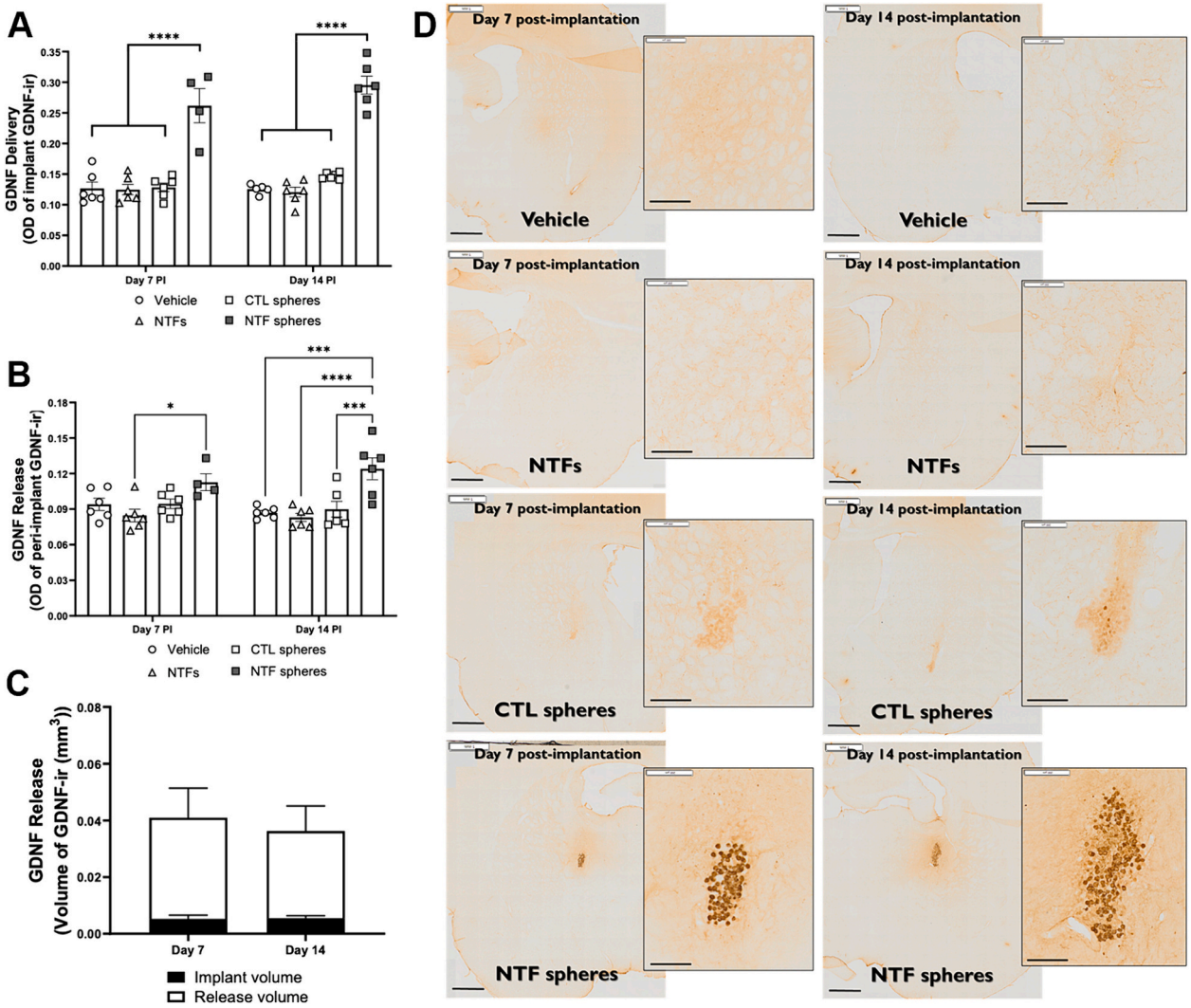

Fig. 12. PEGDA-SPA cryogels deliver GDNF to the brain. GDNF delivery, retention and release from implanted cryogels was assessed by measuring the optical density of GDNF immunostaining at the implant site (A, D) and in the peri-implant region (B, D), as well as the volume of GDNF staining (C, D) at Days 7 and 14 post-implantation. In comparison with bolus administration, GDNF immunostaining was clearly visible both within, and surrounding, the implant site in the brains injected with GDNF-loaded cryogels. Scale bar represents 1 mm and 200 μm (inset). Data are represented as mean ± SEM of $n = 6$ rats. ****$P < 0.0001$, ***$P < 0.001$, *$P < 0.05$ by two-way ANOVA with Tukey *post-hoc* test.

(Fig. 13B; Group, $F_{(3, 38)} = 4.58$, $P < 0.01$). To further assess release, we quantified the volume of striatum into which the neurotrophins had diffused from the neurotrophin-loaded cryogels. This also confirmed release of GDNF (Fig. 12C) and BDNF (Fig. 13C) from the cryogels with the volume of striatum into which the neurotrophins had diffused being much greater than the volume occupied by the implant itself.

Finally, since the cryogels were clearly visible at the implant site, especially when immunostained with GDNF or BDNF, we measured their size *in situ* in the brain to confirm their morphology after *in vivo* implantation (Fig. 14). Cryogels consistently measured ~20 mm (20 ± 0.2 mm) in diameter, and they retained their morphology up to Day 14 after implantation.

4. Discussion

Neurotrophic factors play an essential role in modulating the growth and survival of neurons in the brain, offering potential for neuroprotective and neurorestorative treatments in PD [36]. However, as a recent clinical trial showed, intrastriatal delivery of GDNF requires monthly GDNF infusions over extended time periods [37]. Biomaterial drug delivery systems could be a valuable means of improving local delivery of growth factors to specific brain regions. However, many delivery systems such as PLGA microspheres designed to encapsulate and release proteins have shown an initial burst release where most of the growth factor is released within the first few days [17,38,39]. Another interesting approach involves intranasal delivery of lipid-based nanoparticles to deliver a payload to the midbrain *via* the olfactory system and trigeminal nerve [40,41]. These nanoparticles have been employed for protecting GDNF against degradation and enhance their uptake to the brain in the mouse model of PD [42], particularly when functionalized with the cell-penetrating peptide TAT [43]. Despite the fact that the results were significantly improved, they can rise GDNF expression throughout the whole brain [44]. Therefore, the off-target mediated side-effects may hinder their clinical translation. In this study we aimed to achieve controlled and sustained protein release and move away from stiff polymeric materials to a soft, sponge-like delivery system, for local and minimal invasiveness during implantation.

Cryogel biomaterials can be synthesized to be softer and yet more robust than their hydrogel counterparts [45], compressing and re-expanding to their original shape and size without losing their integrity [21]. This makes them easy to handle and useful as an injectable scaffold for drug delivery to the brain. Unlike the aforementioned

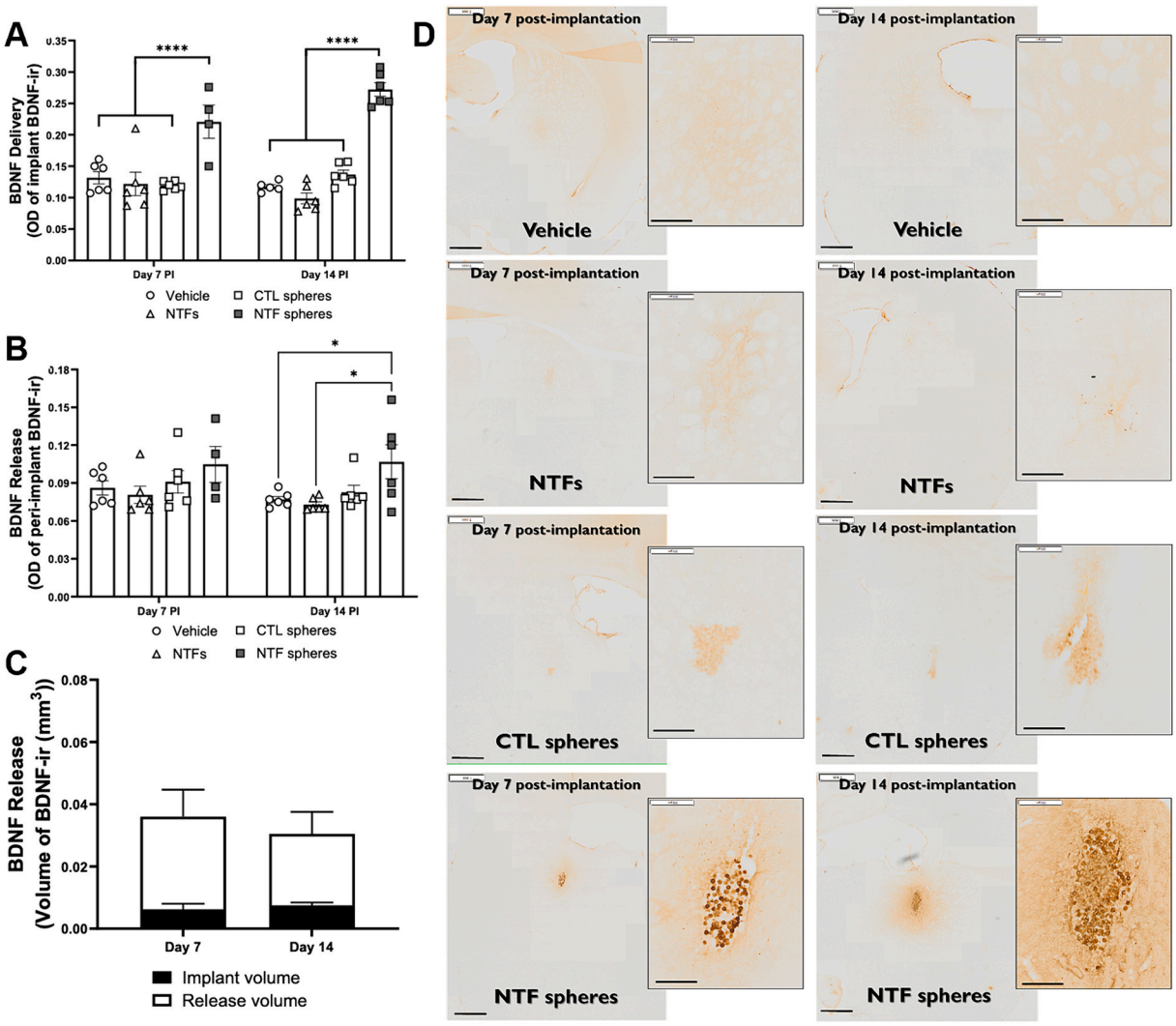

Fig. 13. PEGDA-SPA cryogels deliver BDNF to the brain. BDNF delivery, retention and release from implanted cryogels was assessed by measuring the optical density of BDNF immunostaining at the implant site (A, D) and in the peri-implant region (B, D), as well as the volume of BDNF staining (C, D) at Days 7 and 14 post-implantation. BDNF immunostaining was clearly visible both within, and surrounding, the implant site in the brains injected with BDNF-loaded cryogels though not detectable following a bolus administration. Scale bar represents 1 mm and 200 μm (inset). Data are represented as mean ± SEM of n = 6 rats. ****$P < 0.0001$, *$P < 0.05$ by two-way ANOVA with Tukey *post-hoc* test.

polymeric microspheres, where the payload is encapsulated inside the polymer matrix, cryogels contain interconnected pores where a protein can bind to the surface of the polymer network through electrostatic interactions. Micro-sized cryogels have been successfully fabricated using oil-in-water emulsion methods [46,47] or microscale templates [48,49]. However, here, a microfluidic technology was introduced for scale up and accurate generation of monodisperse cryogel microcarriers.

Affinity-based delivery systems (ABDS) utilize interactions between drugs/proteins and the delivery system to control their loading and release [50]. Heparin has often been incorporated in ABDS to control the release of various drugs/proteins [51,52]. The heparin binding domain on various growth factors is very specific and can interact with heparin *via* non-covalent interactions. Edelman et al. established for the first time a heparin-based delivery system for the controlled release of basic fibroblast growth factor (bFGF) for wound healing and tissue repair applications [53]. Another *in vivo* study evaluated the effect of heparin-based delivery of GDNF from a fibrin matrix on sciatic nerve regeneration for the treatment of peripheral nerve injuries [54]. The system was able to sequester heparin-binding proteins within a fibrin matrix using non-covalent interactions and release it over time. The controlled release of GDNF improved the outgrowth of nerve fibers in the rat sciatic nerve defect. Previously, Newland et al. [47] synthesized 300 μm diameter heparin-based cryogel microcarriers that showed a controlled and sustained release of proteins. However, in our experience, the incorporation of heparin into biomaterial structures has some practical limitations like batch-to-batch variability and unease around potential use in geriatric patients. Instead, using heparin-like moieties within a delivery system can also achieve sustained protein release. For example, Willerth et al. Developed a fibrin matrix containing peptides with affinity for NGF [55]. The release of NGF from the NGF-binding peptide fibrin matrix showed slower release when compared with unmodified fibrin. Since the binding of growth factors is largely due to the highly sulfated nature of heparin, SPA with negatively charged sulfonate moieties was chosen herein to be incorporated into cryogel microcarriers to mimic the protein binding effect of heparin. Our specific objective for this research was to produce negatively charged synthetic cryogel microcarriers that will bind with growth factors through strong electrostatic interaction which then release it in a controlled manner over time.

Interestingly, it seems that BDNF has a greater affinity for the SPA cryogel microcarriers than GDNF, as observed by the higher percentage loading and nearly no release from 95%,80%, 60% and 40% SPA

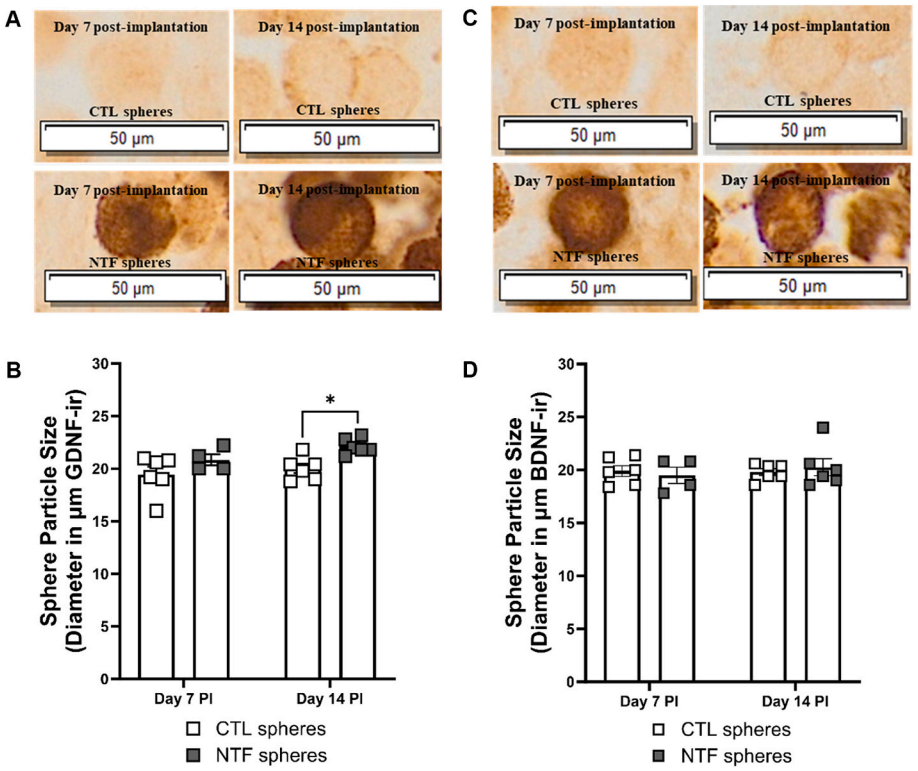

Fig. 14. Morphology of PEGDA-SPA cryogels *in situ* in the brain. The spherical structure of the cryogels was retained after transplantation into the rat striatum. Their size was consistent overall, a small increase in measured diameter was seen in the GDNF-loaded cryogels (A, B) while no change in diameter size in BDNF-loaded cryogels (C, D) at Day 14 after transplantion. Scale bar is 50 μm. Data are represented as mean ± SEM of n = 6 rats (5 cryogels measured per rat). *$P < 0.05$ by two-way ANOVA.

cryogels or very small amount released from 20% or 5% SPA cryogels. Binding affinity is typically measured and described by the equilibrium dissociation constant (K_D), which is used to evaluate different protein-ligand complex interactions [56]. K_D is inversely related to the affinity of the protein for the ligand. As reported in the literature, the K_D value of heparin to BDNF is 1.5×10^{-9} M [57] and to GDNF is 2.27×10^{-8} M [58], indicating that heparin has a higher affinity towards BDNF than GDNF. This may explain the high loading of BDNF and lack of release from the highly sulfonated microcarriers. Moreover, the net charge of the protein at the physiological pH of 7.4 is an important factor. The charge for GDNF and BDNF is 6 and 7.3, respectively (using the protein isoelectric point calculator http://isoelectric.org/calculate.php.) This showed that BDNF has a more positive charge than GDNF, so this also justified the high BDNF loading to the negative cryogel microcarriers.

A new strategy using refillable drug delivery devices is a promising approach for long-term delivery. For example, Nobuhiro Nagai et al., [59] demonstrated the application of the *in situ* gelatin and chitosan gelling system as an ocular injectable drug carrier for sustained and refillable drug delivery systems by reinjection with less invasiveness to intraocular tissues. The release profile of the refilled devices exhibited almost the same rate as that of the first and second refills. Since our cryogels are non-biodegradable, we have tested their ability to be refilled. Our result reinforces the refillable characteristic of the SPA cryogels and thereby highlights their prospective benefit as effective vehicles for controlled and reproducible GDNF delivery.

Biocompatibility is a key necessity for the use of biomaterials in clinical applications. Initially, the cytocompatibility of PEGDA-SPA cryogels was assessed with human neural cell lines and rat primary cell cultures. Several previous studies have shown cryogels and biomaterial polymers composed of PEGDA or SPA to be biocompatible [45,60–63]. In line with this, the SPA cryogels showed no detrimental effects on the metabolic activities of cultures of human neuronal and human microglial cells *in vitro* and rat primary neural cultures *ex vivo*. Additionally, the pronounced benefit of the NTFs released from NTF-loaded cryogels, in line with previous studies [64–68], confirmed that the neurotrophin payload remained functional after binding and release from the sulfonated microcarriers.

One of the future applications of these microcarriers is as an adjuvant to cell transplantation therapy to support cell survival, maturation and integration. Dopamine progenitors typically require GDNF and BDNF for maturation, for at least one month [69]. Therefore, we were interested in maintaining a medium-term release of growth factors for around three months. For that reason, we selected 80% SPA microcarriers for GDNF or 20% SPA microcarriers for BDNF based on the *in vitro* release profile in PBS which showed biologically relevant amounts of protein released over the first month. The doses of GDNF & BDNF were chosen based on our previous studies using primary [7,20] and stem cell-derived [70] dopaminergic neurons.

The *in vivo* biocompatibility of the SPA cryogels was assessed post-implantation in a rat brain. As expected, a transient recruitment of microglia and astrocytes was seen in all the brains as a result of the tissue trauma [71–73], but critically, there was no additional neuro-inflammatory response induced by the cryogels, confirming their biocompatibility.

Given the promising sustained NTF release characteristics shown by the cryogels *in vitro*, we assessed if this translated to sustained release *in vivo* in the brain. SPA cryogels demonstrated their ability to deliver NTFs, retain the delivered cargo, and exhibit sustained release of the retained cargo into the surrounding striatal brain tissue up to 14 days post-implantation, which was in contrast to bolus injection of the proteins. Interestingly, over this period of time, the cryogels themselves were stable in the brain (they did not degrade) and they were still loaded with neurotrophins (based on immunohistochemical staining). This suggests that they could potentially have released the neurotrophins for

longer periods of time (but this was beyond the confines of the present study). This fundamental ability of the SPA cryogels to sustain the availability of NTFs *in vivo* is encouraging, particularly because sustained delivery and release remains one of the key limitations in translating GDNF therapy to the clinic for PD [13]. To date, several strategies for direct protein infusion of GDNF have been assessed in both open label and randomized controlled clinical trials of PD patients (reviewed in [14]). While some of these have shown promise, significant challenges remain, including those related to sustained delivery. Biomaterials, like the PEGDA-SPA cryogel microcarriers reported here, could provide targeted delivery of growth factors in a sustained fashion for extended periods of time.

5. Conclusion

In conclusion, micro-scale cryogels (cryogel microcarriers) could be prepared using a water-in-oil emulsion followed by the cryogelation process. Monodisperse cryogels were successfully developed (20 μm diameter) containing SPA to control the release of growth factors. GDNF and BDNF showed different loading percentages into cryogels with different release profiles depending on the amount of SPA. Moreover, both *in vitro* and *in vivo* studies confirmed biocompatibility and cytocompatibility of theses cryogel microcarriers. After administration into the brain, the microcarriers were able to release GDNF and BDNF in the striatum for two weeks. These small cryogels therefore act as controlled release system for GDNF/BDNF and could therefore increase the therapeutic efficiency of growth factor delivery to the brain. Future studies will evaluate whether the cryogel microcarriers can improve the survival of fetal ventral mesencephalic cells after transplantation into the parkinsonian rat brain model.

CRediT authorship contribution statement

Abrar Hakami: Writing – review & editing, Writing – original draft, Visualization, Validation, Methodology, Investigation, Formal analysis. **Kaushik Narasimhan:** Writing – review & editing, Writing – original draft, Visualization, Validation, Methodology, Investigation, Formal analysis. **Giulia Comini:** Validation, Investigation. **Julian Thiele:** Writing – review & editing, Supervision, Resources, Methodology. **Carsten Werner:** Supervision, Methodology. **Eilís Dowd:** Writing – review & editing, Visualization, Supervision, Resources, Project administration, Methodology, Funding acquisition, Conceptualization. **Ben Newland:** Writing – review & editing, Visualization, Supervision, Resources, Project administration, Methodology, Investigation, Funding acquisition, Conceptualization.

Declaration of competing interest

The authors declare that there are no competing financial interests.

Data availability

Data will be made available on request.

Acknowledgements

AH would like to thank King Abdulaziz University and the Saudi Arabian Ministry of Education for a full PhD scholarship to complete this research at Cardiff University. JT thanks the European Research Council (ERC) under the European Union's Horizon 2020 research and innovation program (Grant agreement No. 852065). ED, KN & GC would like to acknowledge research grants from Science Foundation Ireland (Grant Numbers: 19/FFP/6554) and the Michael J Fox Foundation for Parkinson's Research (Grant Numbers: 17244 and 023410). BN would like to acknowledge the Academy of Medical Sciences, (Springboard Fund - SBF006\1083) for financial support for the study.

Appendix A. Supplementary data

Supplementary data to this article can be found online at https://doi.org/10.1016/j.jconrel.2024.03.023.

References

[1] A.L. Peterson, J.G. Nutt, Treatment of parkinson's disease with trophic factors, Neurotherapeutics 5 (2) (2008) 270–280.
[2] S.J. Allen, J.J. Watson, D.K. Shoemark, N.U. Barua, N.K. Patel, GDNF, NGF and BDNF as therapeutic options for neurodegeneration, Pharmacol. Ther. 138 (2) (2013) 155–175.
[3] S.S. Gill, N.K. Patel, G.R. Hotton, K. O'Sullivan, R. McCarter, M. Bunnage, D. J. Brooks, C.N. Svendsen, P. Heywood, Direct brain infusion of glial cell line-derived neurotrophic factor in parkinson disease, Nat. Med. 9 (5) (2003) 589–595.
[4] M.G. Murer, Q. Yan, R. Raisman-Vozari, Brain-derived neurotrophic factor in the control human brain, and in alzheimer's disease and parkinson's disease, Prog. Neurobiol. 63 (1) (2001) 71–124.
[5] D.M. Gash, G.A. Gerhardt, L.H. Bradley, R. Wagner, J.T. Slevin, GDNF clinical trials for parkinson's disease: a critical human dimension, Cell Tissue Res. 382 (1) (2020) 65–70.
[6] T. Yasuda, H. Mochizuki, Use of growth factors for the treatment of parkinson's disease, Expert. Rev. Neurother. 10 (6) (2010) 915–924.
[7] N. Moriarty, S. Cabre, V. Alamilla, A. Pandit, E. Dowd, Encapsulation of young donor age dopaminergic grafts in a GDNF-loaded collagen hydrogel further increases their survival, reinnervation, and functional efficacy after intrastriatal transplantation in hemi-parkinsonian rats, Eur. J. Neurosci. 49 (4) (2019) 487–496.
[8] L. Feng, C.Y. Wang, H. Jiang, C. Oho, K. Mizuno, M. Dugich-Djordjevic, B. Lu, Differential effects of GDNF and BDNF on cultured ventral mesencephalic neurons, Brain Res. Mol. Brain Res. 66 (1–2) (1999) 62–70.
[9] M. Luz, E. Mohr, H.C. Fibiger, GDNF-induced cerebellar toxicity: a brief review, Neurotoxicology 52 (2016) 46–56.
[10] A.C. Granholm, M. Reyland, D. Albeck, L. Sanders, G. Gerhardt, G. Hoernig, L. Shen, H. Westphal, B. Hoffer, Glial cell line-derived neurotrophic factor is essential for postnatal survival of midbrain dopamine neurons, J. Neurosci. 20 (9) (2000) 3182–3190.
[11] S. Jarrin, A. Hakami, B. Newland, E. Dowd, Growth factor therapy for parkinson's disease: alternative delivery systems, J. Parkinsons Dis. 11 (s2) (2021) S229–S236.
[12] A. Whone, M. Luz, M. Boca, M. Woolley, L. Mooney, S. Dharia, J. Broadfoot, D. Cronin, C. Schroers, N.U. Barua, L. Longpre, C.L. Barclay, C. Boiko, G. A. Johnson, H.C. Fibiger, R. Harrison, O. Lewis, G. Pritchard, M. Howell, C. Irving, D. Johnson, S. Kinch, C. Marshall, A.D. Lawrence, S. Blinder, V. Sossi, A.J. Stoessl, P. Skinner, E. Mohr, S.S. Gill, Randomized trial of intermittent intraputamenal glial cell line-derived neurotrophic factor in Parkinson's disease, Brain 142 (3) (2019) 512–525.
[13] Y.A. Sidorova, M. Saarma, Can growth factors cure parkinson's disease? Trends Pharmacol. Sci. 41 (12) (2020) 909–922.
[14] R.A. Barker, A. Bjorklund, D.M. Gash, A. Whone, A. Van Laar, J.H. Kordower, K. Bankiewicz, K. Kieburtz, M. Saarma, S. Booms, H.J. Huttunen, A.P. Kells, M. S. Fiandaca, A.J. Stoessl, D. Eidelberg, H. Federoff, M.H. Voutilainen, D.T. Dexter, J. Eberling, P. Brundin, L. Isaacs, L. Mursaleen, E. Bresolin, C. Carroll, A. Coles, B. Fiske, H. Matthews, C. Lungu, R.K. Wyse, S. Stott, A.E. Lang, GDNF and parkinson's disease: where next? A summary from a recent workshop, J. Parkinsons Dis. 10 (3) (2020) 875–891.
[15] P.V. Torres-Ortega, L. Saludas, A.S. Hanafy, E. Garbayo, M.J. Blanco-Prieto, Micro- and nanotechnology approaches to improve parkinson's disease therapy, J. Control. Release 295 (2019) 201–213.
[16] B. Newland, H. Newland, C. Werner, A. Rosser, W. Wang, Prospects for polymer therapeutics in parkinson's disease and other neurodegenerative disorders, Prog. Polym. Sci. 44 (2015) 79–112.
[17] E. Garbayo, C.N. Montero-Menei, E. Ansorena, J.L. Lanciego, M.S. Aymerich, M. J. Blanco-Prieto, Effective GDNF brain delivery using microspheres–a promising strategy for parkinson's disease, J. Control. Release 135 (2) (2009) 119–126.
[18] E. Garbayo, E. Ansorena, H. Lana, M.D. Carmona-Abellan, I. Marcilla, J. L. Lanciego, M.R. Luquin, M.J. Blanco-Prieto, Brain delivery of microencapsulated GDNF induces functional and structural recovery in parkinsonian monkeys, Biomaterials 110 (2016) 11–23.
[19] S.D. Allison, Analysis of initial burst in PLGA microparticles, Expert Opin. Drug Deliv. 5 (6) (2008) 615–628.
[20] N. Moriarty, A. Pandit, E. Dowd, Encapsulation of primary dopaminergic neurons in a GDNF-loaded collagen hydrogel increases their survival, re-innervation and function after intra-striatal transplantation, Sci. Rep. 7 (1) (2017) 16033.
[21] S.A. Bencherif, R.W. Sands, D. Bhatta, P. Arany, C.S. Verbeke, D.A. Edwards, D. J. Mooney, Injectable preformed scaffolds with shape-memory properties, Proc. Natl. Acad. Sci. USA 109 (48) (2012) 19590–19595.
[22] S.T. Koshy, D.K. Zhang, J.M. Grolman, A.G. Stafford, D.J. Mooney, Injectable nanocomposite cryogels for versatile protein drug delivery, Acta Biomater. 65 (2018) 36–43.
[23] Y. Saylan, A. Denizli, Supermacroporous composite cryogels in biomedical applications, Gels 5 (2) (2019) 20.
[24] H. Kirsebom, G. Rata, D. Topgaard, B. Mattiasson, I.Y. Galaev, Mechanism of Cryopolymerization: diffusion-controlled polymerization in a nonfrozen microphase. An NMR study, Macromolecules 42 (14) (2009) 5208–5214.

[25] I. Alfano, P. Vora, R.S. Mummery, B. Mulloy, C.C. Rider, The major determinant of the heparin binding of glial cell-line-derived neurotrophic factor is near the N-terminus and is dispensable for receptor binding, Biochem. J. 404 (1) (2007) 131–140.
[26] A.M. Sandoval-Castellanos, F. Claeyssens, J.W. Haycock, Biomimetic surface delivery of NGF and BDNF to enhance neurite outgrowth, Biotechnol. Bioeng. 117 (10) (2020) 3124–3135.
[27] Y. Ma, J. Thiele, L. Abdelmohsen, J. Xu, W.T. Huck, Biocompatible macro-initiators controlling radical retention in microfluidic on-chip photo-polymerization of water-in-oil emulsions, Chem. Commun. (Camb.) 50 (1) (2014) 112–114.
[28] M.J. Männel, L. Selzer, R. Bernhardt, J. Thiele, Optimizing process parameters in commercial micro-stereolithography for forming emulsions and polymer microparticles in nonplanar microfluidic devices, Adv. Mater. Technol. 4 (1) (2019) 1800408.
[29] B. Newland, M. Abu-Rub, M. Naughton, Y. Zheng, A.V. Pinoncely, E. Collin, E. Dowd, W. Wang, A. Pandit, GDNF gene delivery via a 2-(dimethylamino)ethyl methacrylate based cyclized knot polymer for neuronal cell applications, ACS Chem. Neurosci. 4 (4) (2013) 540–546.
[30] B. Newland, T.C. Moloney, G. Fontana, S. Browne, M.T. Abu-Rub, E. Dowd, A. S. Pandit, The neurotoxicity of gene vectors and its amelioration by packaging with collagen hollow spheres, Biomaterials 34 (8) (2013) 2130–2141.
[31] B. Newland, H. Newland, F. Lorenzi, D. Eigel, P.B. Welzel, D. Fischer, W. Wang, U. Freudenberg, A. Rosser, C. Werner, Injectable glycosaminoglycan-based cryogels from well-defined microscale templates for local growth factor delivery, ACS Chem. Neurosci. 12 (7) (2021) 1178–1188.
[32] S.B. Dunnett, A. Bjorklund, Basic neural transplantation techniques. I. Dissociated cell suspension grafts of embryonic ventral mesencephalon in the adult rat brain, Brain Res. Brain Res. Protoc. 1 (1) (1997) 91–99.
[33] C. Naughton, N. Moriarty, J. Feehan, D. O'Toole, E. Dowd, Differential pattern of motor impairments in neurotoxic, environmental and inflammation-driven rat models of parkinson's disease, Behav. Brain Res. 296 (2016) 451–458.
[34] D.B. Hoban, B. Newland, T.C. Moloney, L. Howard, A. Pandit, E. Dowd, The reduction in immunogenicity of neurotrophin overexpressing stem cells after intra-striatal transplantation by encapsulation in an in situ gelling collagen hydrogel, Biomaterials 34 (37) (2013) 9420–9429.
[35] Y. Garcia, A. Breen, K. Burugapalli, P. Dockery, A. Pandit, Stereological methods to assess tissue response for tissue-engineered scaffolds, Biomaterials 28 (2) (2007) 175–186.
[36] W. Poewe, The natural history of parkinson's disease, J. Neurol. 253 (7) (2006) vii2–vii6.
[37] J.T. Slevin, D.M. Gash, C.D. Smith, G.A. Gerhardt, R. Kryscio, H. Chebrolu, A. Walton, R. Wagner, A.B. Young, Unilateral intraputamenal glial cell line-derived neurotrophic factor in patients with parkinson disease: response to 1 year of treatment and 1 year of withdrawal, J. Neurosurg. 106 (4) (2007) 614–620.
[38] A. Aubert-Pouessel, M.C. Venier-Julienne, A. Clavreul, M. Sergent, C. Jollivet, C. N. Montero-Menei, E. Garcion, D.C. Bibby, P. Menei, J.P. Benoit, In vitro study of GDNF release from biodegradable PLGA microspheres, J. Control. Release 95 (3) (2004) 463–475.
[39] C.E. Witherel, K. Sao, B.K. Brisson, B. Han, S.W. Volk, R.J. Petrie, L. Han, K. L. Spiller, Regulation of extracellular matrix assembly and structure by hybrid M1/M2 macrophages, Biomaterials 269 (2021) 120667.
[40] S. Rehman, B. Nabi, A. Zafar, S. Baboota, J. Ali, Intranasal delivery of mucoadhesive nanocarriers: a viable option for parkinson's disease treatment? Expert Opin. Drug Deliv. 16 (12) (2019) 1355–1366.
[41] A.D. Kulkarni, Y.H. Vanjari, K.H. Sancheti, V.S. Belgamwar, S.J. Surana, C. V. Pardeshi, Nanotechnology-mediated nose to brain drug delivery for parkinson's disease: a mini review, J. Drug Target. 23 (9) (2015) 775–788.
[42] O. Gartziandia, E. Herrán, J. Ruiz-Ortega, C. Miguelez, M. Igartua, J. Lafuente, J. Pedraz, L. Ugedo, R. Hernández, Intranasal administration of chitosan-coated nanostructured lipid carriers loaded with GDNF improves behavioral and histological recovery in a partial lesion model of parkinson's disease, J. Biomed. Nanotechnol. 12 (12) (2016) 2220–2280.
[43] S. Hernando, E. Herran, J. Figueiro-Silva, J.L. Pedraz, M. Igartua, E. Carro, R. M. Hernandez, Intranasal administration of TAT-conjugated lipid nanocarriers loading GDNF for parkinson's disease, Mol. Neurobiol. 55 (2018) 145–155.
[44] T. Bender, M. Migliore, R. Campbell, S.J. Gatley, B. Waszczak, Intranasal administration of glial-derived neurotrophic factor (GDNF) rapidly and significantly increases whole-brain GDNF level in rats, Neuroscience 303 (2015) 569–576.
[45] D. Eigel, R. Schuster, M.J. Mannel, J. Thiele, M.J. Panasiuk, L.C. Andreae, C. Varricchio, A. Brancale, P.B. Welzel, W.B. Huttner, C. Werner, B. Newland, K. R. Long, Sulfonated cryogel scaffolds for focal delivery in ex-vivo brain tissue cultures, Biomaterials 271 (2021) 120712.
[46] P. Xia, K. Zhang, Y. Gong, G. Li, S. Yan, J. Yin, Injectable stem cell laden open porous microgels that favor adipogenesis: in vitro and in vivo evaluation, ACS Appl. Mater. Interfaces 9 (40) (2017) 34751–34761.
[47] B. Newland, P.B. Welzel, H. Newland, C. Renneberg, P. Kolar, M. Tsurkan, A. Rosser, U. Freudenberg, C. Werner, Tackling cell transplantation anoikis: an injectable, shape memory cryogel microcarrier platform material for stem cell and neuronal cell growth, Small 11 (38) (2015) 5047–5053.
[48] Y. Zeng, C. Chen, W. Liu, Q. Fu, Z. Han, Y. Li, S. Feng, X. Li, C. Qi, J. Wu, D. Wang, C. Corbett, B.P. Chan, D. Ruan, Y. Du, Injectable microcryogels reinforced alginate encapsulation of mesenchymal stromal cells for leak-proof delivery and alleviation of canine disc degeneration, Biomaterials 59 (2015) 53–65.
[49] Y. Zeng, L. Zhu, Q. Han, W. Liu, X. Mao, Y. Li, N. Yu, S. Feng, Q. Fu, X. Wang, Y. Du, R.C. Zhao, Preformed gelatin microcryogels as injectable cell carriers for enhanced skin wound healing, Acta Biomater. 25 (2015) 291–303.
[50] N.X. Wang, H.A. von Recum, Affinity-based drug delivery, Macromol. Biosci. 11 (3) (2011) 321–332.
[51] B. Newland, C. Varricchio, Y. Korner, F. Hoppe, C. Taplan, H. Newland, D. Eigel, G. Tornillo, D. Pette, A. Brancale, P.B. Welzel, F.P. Seib, C. Werner, Focal drug administration via heparin-containing cryogel microcarriers reduces cancer growth and metastasis, Carbohydr. Polym. 245 (2020) 116504.
[52] L. Schirmer, C. Hoornaert, D. Le Blon, D. Eigel, C. Neto, M. Gumbleton, P.B. Welzel, A.E. Rosser, C. Werner, P. Ponsaerts, B. Newland, Heparin-based, injectable microcarriers for controlled delivery of interleukin-13 to the brain, Biomater. Sci. 8 (18) (2020) 4997–5004.
[53] E.R. Edelman, E. Mathiowitz, R. Langer, M. Klagsbrun, Controlled and modulated release of basic fibroblast growth factor, Biomaterials 12 (7) (1991) 619–626.
[54] M.D. Wood, A.M. Moore, D.A. Hunter, S. Tuffaha, G.H. Borschel, S.E. Mackinnon, S.E. Sakiyama-Elbert, Affinity-based release of glial-derived neurotrophic factor from fibrin matrices enhances sciatic nerve regeneration, Acta Biomater. 5 (4) (2009) 959–968.
[55] S.M. Willerth, P.J. Johnson, D.J. Maxwell, S.R. Parsons, M.E. Doukas, S. E. Sakiyama-Elbert, Rationally designed peptides for controlled release of nerve growth factor from fibrin matrices, J. Biomed. Mater. Res. A 80 (1) (2007) 13–23.
[56] J. Corzo, Time, the forgotten dimension of ligand binding teaching, Biochem. Mol. Biol. Educ. 34 (6) (2006) 413–416.
[57] Y. Kanato, S. Ono, K. Kitajima, C. Sato, Complex formation of a brain-derived neurotrophic factor and glycosaminoglycans, Biosci. Biotechnol. Biochem. 73 (12) (2009) 2735–2741.
[58] M.M. Bespalov, Y.A. Sidorova, S. Tumova, A. Ahonen-Bishopp, A.C. Magalhaes, E. Kulesskiy, M. Paveliev, C. Rivera, H. Rauvala, M. Saarma, Heparan sulfate proteoglycan syndecan-3 is a novel receptor for GDNF, neurturin, and artemin, J. Cell Biol. 192 (1) (2011) 153–169.
[59] N. Nagai, S. Saijo, Y. Song, H. Kaji, T. Abe, A drug refillable device for transscleral sustained drug delivery to the retina, Eur. J. Pharm. Biopharm. 136 (2019) 184–191.
[60] X. Li, Z. Yuan, X. Wei, H. Li, G. Zhao, J. Miao, D. Wu, B. Liu, S. Cao, D. An, W. Ma, H. Zhang, W. Wang, Q. Wang, H. Gu, Application potential of bone marrow mesenchymal stem cell (BMSCs) based tissue-engineering for spinal cord defect repair in rat fetuses with spina bifida aperta, J. Mater. Sci. Mater. Med. 27 (4) (2016) 77.
[61] N. Rekowska, M. Teske, D. Arbeiter, A. Brietzke, J. Konasch, A. Riess, R. Mau, T. Eickner, H. Seitz, N. Grabow, Biocompatibility and thermodynamic properties of PEGDA and two of its copolymer, Annu. Int. Conf. IEEE Eng. Med. Biol. Soc. 2019 (2019) 1093–1096.
[62] K. McAvoy, D. Jones, R.R.S. Thakur, Synthesis and characterisation of photocrosslinked poly(ethylene glycol) diacrylate implants for sustained ocular drug delivery, Pharm. Res. 35 (2) (2018) 36.
[63] M. Burattini, R. Lippens, N. Baleine, M. Gerard, J. Van Meerssche, C. Geeroms, J. Odent, J.M. Raquez, S. Van Vlierberghe, L. Thorrez, Ionically modified gelatin hydrogels maintain murine myogenic cell viability and fusion capacity, Macromol. Biosci. 23 (7) (2023) e2300019.
[64] L.F. Lin, D.H. Doherty, J.D. Lile, S. Bektesh, F. Collins, GDNF: a glial cell line-derived neurotrophic factor for midbrain dopaminergic neurons, Science 260 (5111) (1993) 1130–1132.
[65] L.F. Lin, T.J. Zhang, F. Collins, L.G. Armes, Purification and initial characterization of rat B49 glial cell line-derived neurotrophic factor, J. Neurochem. 63 (2) (1994) 758–768.
[66] B. Knusel, J.W. Winslow, A. Rosenthal, L.E. Burton, D.P. Seid, K. Nikolics, F. Hefti, Promotion of central cholinergic and dopaminergic neuron differentiation by brain-derived neurotrophic factor but not neurotrophin 3, Proc. Natl. Acad. Sci. USA 88 (3) (1991) 961–965.
[67] C. Hyman, M. Hofer, Y.A. Barde, M. Juhasz, G.D. Yancopoulos, S.P. Squinto, R. M. Lindsay, BDNF is a neurotrophic factor for dopaminergic neurons of the substantia nigra, Nature 350 (6315) (1991) 230–232.
[68] L. Studer, C. Spenger, R.W. Seiler, C.A. Altar, R.M. Lindsay, C. Hyman, Comparison of the effects of the neurotrophins on the morphological structure of dopaminergic neurons in cultures of rat substantia nigra, Eur. J. Neurosci. 7 (2) (1995) 223–233.
[69] S. Nolbrant, A. Heuer, M. Parmar, A. Kirkeby, Generation of high-purity human ventral midbrain dopaminergic progenitors for in vitro maturation and intracerebral transplantation, Nat. Protoc. 12 (9) (2017) 1962–1979.
[70] C. Comini, R. Kelly, S. Jarrin, T. Patton, K. Narasimhan, A. Pandit, N. Drummond, T. Kunath, E. Dowd, Survival and maturation of human induced pluripotent stem cell-derived dopaminergic progenitors in the parkinsonian rat brain is enhanced by transplantation in a neurotrophin-enriched hydrogel, J. Neural Eng. (2024), https://doi.org/10.1088/1741-2552/ad33b2 (in press).
[71] R.A. Barker, S.B. Dunnett, A. Faissner, J.W. Fawcett, The time course of loss of dopaminergic neurons and the gliotic reaction surrounding grafts of embryonic mesencephalon to the striatum, Exp. Neurol. 141 (1) (1996) 79–93.
[72] N. Tomov, L. Surchev, C. Wiedenmann, M. Dobrossy, G. Nikkhah, Roscovitine, an experimental CDK5 inhibitor, causes delayed suppression of microglial, but not astroglial recruitment around intracerebral dopaminergic grafts, Exp. Neurol. 318 (2019) 135–144.
[73] N. Tomov, Glial cells in intracerebral transplantation for parkinson's disease, Neural Regen. Res. 15 (7) (2020) 1173–1178.